Journal of Medicinal Chemistry

Article

Increasing C-Terminal Hydrophobicity Improves the Cell Permeability and Antiproliferative Activity of PACE4 Inhibitors against Prostate Cancer Cell Lines

Vahid Dianati, Anna Kwiatkowska, Frédéric Couture, Roxane Desjardins, Yves L. Dory, and Robert Day

J. Med. Chem., **Just Accepted Manuscript** • DOI: 10.1021/acs.jmedchem.8b01144 • Publication Date (Web): 05 Sep 2018

ACS Publications

is published by the American Chemical Society. 1155 Sixteenth Street N.W., Washington, DC 20036

Increasing C-Terminal Hydrophobicity Improves the Cell Permeability and Antiproliferative Activity of PACE4 Inhibitors against Prostate Cancer Cell Lines

*Vahid Dianati,[†] Anna Kwiatkowska,[‡] Frédéric Couture,[‡] Roxane Desjardins,[‡] Yves L. Dory[†]*and Robert Day[‡]**

†Institut de Pharmacologie de Sherbrooke, Département de Chimie, Faculté des Sciences, Université de Sherbrooke, 3001, 12e Avenue Nord, Sherbrooke, Québec, J1H 5N4 (Canada)

‡Institut de Pharmacologie de Sherbrooke, Département de Chirurgie/Urologie, Université de Sherbrooke, 3001, 12e Avenue Nord, Sherbrooke, Québec,

J1H 5N4 (Canada)

KEYWORDS. Prostate cancer, Proprotein convertases, PACE4, Inhibitor, Cell permeability, Cell penetrating peptide.

ABSTRACT

The serine protease, PACE4, is a proprotein convertase which plays a substantial role in malignancy of prostate cancer. Our initial selective PACE4 inhibitor (Ac-LLLLRVKR-NH_2) has evolved to our current lead compound C23 (Ac-DLeu-LLLRVK-Amba), which is active both in-

vitro and in-vivo. By screening natural residues, except Cys, in C-terminal P1' position, it was established that increasing hydrophobicity was improving cell permeability, which was directly translated into PCa cells antiproliferative activity. This cell antiproliferation enhancement seems independent from effect of P1' residue on PACE4 affinity. Replacement of P1-Amba of C23 by Acpa ((*S*)-2-amino-3-(4-carbamimidoylphenyl)propanoic acid) followed by addition of tryptamine in P1' resulted in compound **32** exhibiting superior PCa cells antiproliferative activity over the reference compound C23 (3-fold). This study sheds light on key factors that improve cell penetrating property and antiproliferative activity of PACE4 inhibitors.

INTRODUCTION

PACE4 is an enzyme in the family of proprotein convertases (PCs) that activates secretory protein precursors through peptide bond cleavage at paired basic amino acids (i.e., consensus cleavage site R-X-R/K-R↓). PACE4 transits within the secretory pathway and is secreted.[1-2] Our studies were the first to demonstrate the role of PACE4 in prostate cancer (PCa).[3] We showed an overexpression of PACE4 in PCa tissues obtained from patients who underwent radical prostatectomy for clinically localized tumor, while no other PC showed any significant changes. Using mouse PCa xenograft models, we also showed that only PACE4 inhibition blocks PCa progression, and not the inhibition of other PCs.[4] Recently, we discovered that PCa cells utilize an alternative splicing mechanism to generate a cancer-specific C-terminally modified PACE4 isoform (named PACE4-altCT), which is retained in the cell.[5] RNA interference silencing studies targeting PACE4-altCT demonstrate that this isoform is responsible for PACE4-associated cancer progression. PACE4 is also overexpressed and involved in other malignancy including non-small cell lung carcinoma, ovarian, and breast cancer.[3-4, 6-8] The sum of our data

provides the proof of concept and the justification to proceed with a development plan for PACE4 inhibitors for a novel cancer therapy.

In this regard, we developed a specific PACE4 inhibitor named the Multi-Leu peptide (ML-peptide).[9-10] In enzyme kinetic assays, the ML-peptide (sequence: Ac-LLLLRVKR-NH_2) **1** is potent (K_i = 22 ± 6 nM) and selective for PACE4 (e.g., 20-fold over furin). In cell-based assays, the compound **1** blocks the proliferation of PCa cell lines (LNCaP, DU145 and 22Rv1) and induces G_0/G_1 cell cycle arrest. We also discovered that the target of the compound **1** is intracellular since a cell impermeable analog (i.e., PEG8-ML-peptide) has no effect on cell proliferation.[9] We believe compound **1** exerts its anti-proliferative effects by reaching PACE4-altCT (i.e., cell retained PACE4 isoform). While potent in cell-based assays, the compound **1** displays poor stability in vivo, so we developed a stable version named C23 (compound **2**; **Figure 1**).[11] Among the modifications in compound **2**, the replacement of the P1 Arg by 4-amidinobenzylamide (Amba) gives this PACE4 inhibitor with higher potency than the compound **1** and antiproliferative activity against PCa cell lines and improved stability and pharmacokinetic profile.[10, 12-13] The additional change of P8-Leu to its D-isomer, raised the plasma stability up to 1.7 hours with almost no loss of potency and anti-proliferative activity.[12,14] In LNCaP xenografted mice, compound **2** (2 mg/kg/day iv) diminished tumor volumes by 60% over 18 days with a 47% reduction in plasma PSA levels, as well as a significant decrease in cells progressing through the cell cycle, increased apoptosis and impaired neovascularization.[11]

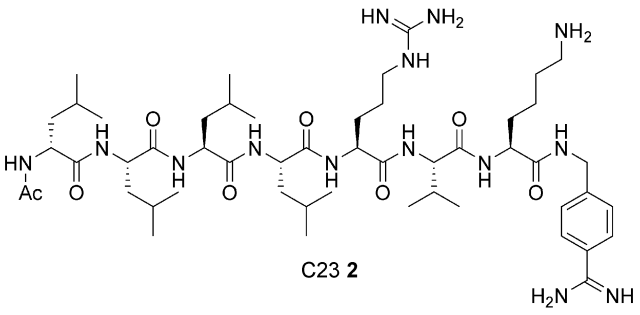

C23 **2**

Figure 1. Structure of lead compound **2** (C23)

While compound **2** represents a significant improvement for PACE4 inhibition in vivo, further refinements may be needed. Indeed, a systematic scan of positions P5 to P8 of compound **2** revealed that these four residues have to be hydrophobic. It was even shown that charged residues at those positions reduce antiproliferative activity on PCa cell lines. This may be due to the disruption of the amphipathic nature of the inhibitor, which affects its cell penetrating properties.[15] Parallel studies on the compound **1** indicated that introduction of a β-branched basic residue, (2*S*)-amino-(3*S*)-guanidinobutyryl (*S*-*i*-Agb), in the P3 position led to a compound with unprecedented high potency and selectivity towards PACE4.[16] However, further antiproliferative PCa cells analysis of this compound and related analogs showed very poor activity.

The analysis of PC homology models based on furin crystal structure suggests that the S1 to S4 pockets are strongly conserved among PCs.[17] However, these models also highlight noticeable differences in the P' region of PC catalytic pockets. Despite few reports, no comprehensive investigation has been done on the significance of the P' region of the catalytic site for PACE4 inhibitors.[18-19] Accordingly, a screening was conducted with natural residues at the P1' position of the compound **1**. The impact of these modifications was evaluated on the inhibition of PACE4 and PCa cell lines antiproliferative activity of new compounds. Additional

molecules were further designed based on the obtained results to evaluate any potential gain in terms of PACE4 inhibition and cellular activity.

RESULTS AND DISCUSSION

Screening of DNA-encoded residues in P1'. So far, the most potent PACE4 inhibitors including our lead compound **2** have been armed with Amba at their P1 C-terminal. For synthetic feasibility reasons in the investigation of the P1' position, Amba was replaced by Arg-NH_2. The 20 natural amino acids, except Cys, have been incorporated in the P1' position of compound **1**. The inhibitory constants (K_i) of each peptide have been determined for PACE4 and furin using a fluorometric assay to compare the binding affinities. The efficacy of compounds was further assessed ex vivo using DU145 and LNCaP PCa cell lines using an MTT cell proliferation assay.

The PACE4 and furin affinities (**Table 1**) of the new compounds **3**−**21**, compared to the control compounds **1** and **2**, reveal that P1'-Lys (**10**) and P1'-Arg (**16**) are the least-favored residues for the S1' pocket of both enzyme which is in accordance with what has been observed for affinity of PC's substrates.[17] However, only compounds **10** and **16** remain as selective as compound **1** (17 and 16 times more selective toward PACE4, respectively). As illustrated in **Figure 2**, other P1'-modified peptides, except Pro (**14**) and Leu (**11**), inhibit PACE4 in the range of compound **1** (20-64 nM). Compounds **6**, **20** and **21** with aromatic residues (Phe, Trp and Tyr) in P1' are among the best PACE4 inhibitors in this series, with compound **6** displaying a K_i value as low as 20 ± 2 nM for PACE4. In general, most of the inhibitors were showing enhanced affinity for furin and diminished inhibition of PACE4, in comparison to compound **1**. As a result, no gain in selectivity was ever observed with the introduction of residues in position P1'. The PACE4 inhibition profile of compounds **3**−**21** suggests that no natural residue could introduce a favorable interaction with PACE4 in the S1' pocket.

Table 1. Inhibition profiles and cellular antiproliferative activities of compounds **3**−**21** with general structure of Ac-Leu-Leu-Leu-Leu-Arg-Val-Lys-Xaa-NH_2 compared to control compounds **1** and **2**

Entry	Structure	K_i (nM) ± SEM[a]		Selectivity for PACE4	IC_{50} (μM) ± SEM[a]	
		PACE4	Furin		DU145	LNCaP
1	Ac-Leu-Leu-Leu-Leu-Arg-Val-Lys-Arg-NH_2[b]	22 ± 6	430 ± 10	20	100 ± 10	180 ± 60
2	Ac-**DLeu**-Leu-Leu-Leu-Arg-Val-Lys-**Amba**[b]	4.9 ± 0.9	9.8 ± 2	2	25 ± 10	45 ± 10
3	Ac-Leu-Leu-Leu-Leu-Arg-Val-Lys-Arg-**Ala**-NH_2	37 ± 5	210±10	6	160 ± 10	N.D.[c]
4	Ac-Leu-Leu-Leu-Leu-Arg-Val-Lys-Arg-**Asp**-NH_2	30 ± 2	74 ± 8	2	230 ± 20	N.D.
5	Ac-Leu-Leu-Leu-Leu-Arg-Val-Lys-Arg-**Glu**-NH_2	58 ± 4	260 ± 30	4	N.C.[d]	N.D.
6	Ac-Leu-Leu-Leu-Leu-Arg-Val-Lys-Arg-**Phe**-NH_2	20 ± 2	74 ± 9	4	70 ± 8	170 ± 40
7	Ac-Leu-Leu-Leu-Leu-Arg-Val-Lys-Arg-**Gly**-NH_2	44 ± 5	500 ± 30	11	N.C.	N.D.
8	Ac-Leu-Leu-Leu-Leu-Arg-Val-Lys-Arg-**His**-NH_2	33 ± 7	140 ± 10	4	N.C.	N.D.
9	Ac-Leu-Leu-Leu-Leu-Arg-Val-Lys-Arg-**Ile**-NH_2	64 ± 4	290 ± 10	5	72 ± 8	N.C.
10	Ac-Leu-Leu-Leu-Leu-Arg-Val-Lys-Arg-**Lys**-NH_2	150 ± 20	2600 ± 100	17	130 ± 10	N.D.
11	Ac-Leu-Leu-Leu-Leu-Arg-Val-Lys-Arg-**Leu**-NH_2	170 ± 30	990 ± 30	6	90 ± 10	N.D.
12	Ac-Leu-Leu-Leu-Leu-Arg-Val-Lys-Arg-**Met**-NH_2	32 ± 2	170 ± 10	5	130 ± 20	N.D.
13	Ac-Leu-Leu-Leu-Leu-Arg-Val-Lys-Arg-**Asn**-NH_2	28 ± 3	130 ± 20	5	N.C.	N.D.
14	Ac-Leu-Leu-Leu-Leu-Arg-Val-Lys-Arg-**Pro**-NH_2	250 ± 10	990 ± 30	4	210 ± 30	N.D.
15	Ac-Leu-Leu-Leu-Leu-Arg-Val-Lys-Arg-**Gln**-NH_2	43 ± 3	190 ± 10	5	210 ± 20	N.D.
16	Ac-Leu-Leu-Leu-Leu-Arg-Val-Lys-Arg-**Arg**-NH_2	160 ± 5	2500 ± 400	16	71 ± 7	N.C.
17	Ac-Leu-Leu-Leu-Leu-Arg-Val-Lys-Arg-**Ser**-NH_2	64 ± 2	330 ± 20	5	240 ± 50	N.D.
18	Ac-Leu-Leu-Leu-Leu-Arg-Val-Lys-Arg-**Thr**-NH_2	22 ± 2	100 ± 10	5	170 ± 10	N.D.
19	Ac-Leu-Leu-Leu-Leu-Arg-Val-Lys-Arg-**Val**-NH_2	38 ± 4	200 ± 10	5	170 ± 10	N.D.
20	Ac-Leu-Leu-Leu-Leu-Arg-Val-Lys-Arg-**Trp**-NH_2	29 ± 1	110 ± 10	4	25 ± 2	31 ± 3
21	Ac-Leu-Leu-Leu-Leu-Arg-Val-Lys-Arg-**Tyr**-NH_2	29 ± 1	64 ± 5	2	100 ± 20	N.D.

[a]K_i and IC_{50} values are based on at least two independent experiments. Errors reported as SEM for K_i and IC_{50}. For more details of inhibitor concentrations used in the MTT antiproliferative assay see experimental section. [b]Data were adapted from references 10 and 12. [c]N.D.: Not determined. [d]N.C.: Not calculable as the curves did not converge to 50% with doses up to 300 μM.

MTT cell proliferation was then investigated to assess the cell activity of inhibitors on PCa cell lines (**Table 1**). The compounds **3**−**21** were first monitored on DU145 cells. Thereafter, the most active compounds were also examined on LNCaP cells. Clearly, the introduction of hydrophobic residues in P1' position enhances the antiproliferative activity of peptides. For instance, compounds with P1' residues Phe (**6**), Ile (**9**), Leu (**11**) and Trp (**20**) led to the IC_{50} values of 70 ± 8, 72 ± 8, 90 ± 10 and 24 ± 2 μM, for DU145 PCa cells, respectively. As exceptions for polar residues, we were at first very surprised by the P1'-Lys (**10**) and P1'-Arg (**16**) peptides with their respective antiproliferative IC_{50} values of 130 ± 20 and 71 ± 7 μM while they are very weak PACE4 inhibitors. Based on these results, it was then uncovered that positive charge and hydrophobicity in P1' residue are the main factors for enhancing the antiproliferative activity.

SAR studies based on the screening. Following the encouraging data collected for peptides **6**, **16** and **20** (**Table 1**), the next logical move was to combine the basic nature of Arg and the aromatic nature of Phe at position P1'. This is how the new residues 4-aminophenylalanine (Apa) **22**, 4-guanidinophenylalanine (Gpa) **23** and 4-(2-aminoethyl)benzimidamide (Aeba) **24** were designed (**Figure 2-a**). Hence, the corresponding compounds **28**−**30** were synthesized on solid support, then tested (**Figure 2-b**). Only compound **29** inhibited PACE4 with an improved K_i of 11 ± 2 nM but once again, this increased affinity didn't translate to antiproliferative activity. The reduced polarity in Aeba **24** with no C-terminal $-CONH_2$ group, contributed to the antiproliferative properties of compound **30** (41 ± 9 and 67 ± 7 μM for DU145 and LNCaP cells, respectively) which is no better than lead compound **2**.

a)

Entry	Structure	K_i (nM) ± SEM		Selectivity for PACE4	IC_{50} (μM) ± SEM	
		PACE4	Furin		DU145	LNCaP
28	Ac-Leu-Leu-Leu-Leu-Arg-Val-Lys-Arg-**Apa**-NH_2	32 ± 4	130 ± 10	4	139 ± 4	170 ± 10
29	Ac-Leu-Leu-Leu-Leu-Arg-Val-Lys-Arg-**Gpa**-NH_2	11 ± 2	140 ± 10	13	83 ± 2	92 ± 2
30	Ac-**D**Leu-Leu-Leu-Leu-Arg-Val-Lys-Arg-**Aeba**	68 ± 1	700 ± 100	10	41 ± 9	67 ± 7
31	Ac-**D**Leu-Leu-Leu-Leu-Arg-Val-Lys-Arg-**Tryp**	70 ± 10	280 ± 2	4	14 ± 2	18 ± 5
32	Ac-**D**Leu-Leu-Leu-Leu-Arg-Val-Lys-Arg-**Acpa-Tryp**	41 ± 5	80 ± 10	2	7.5 ± 0.8	13 ± 1
33	Ac-**D**Leu-Leu-Leu-Leu-Arg-Val-Lys-Arg-**Aca-Tryp**	248 ± 6	3000 ± 500	12	40 ± 20	70 ± 20

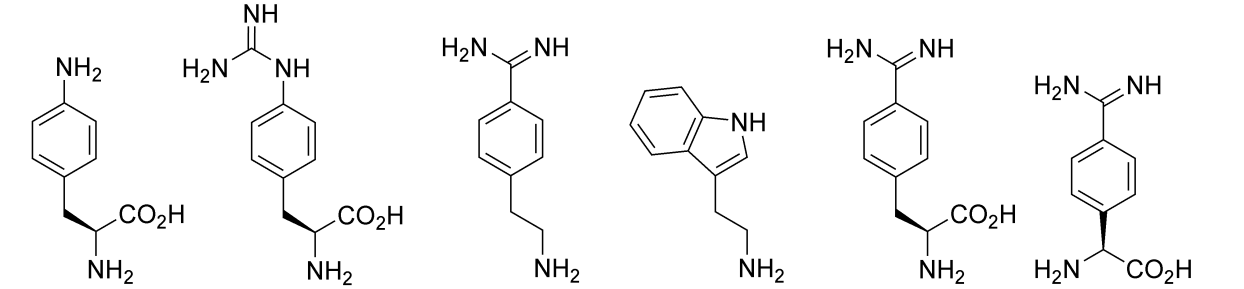

Apa **22** Gpa **23** Aeba **24** Tryp **25** Acpa **26** Aca **27**

b)

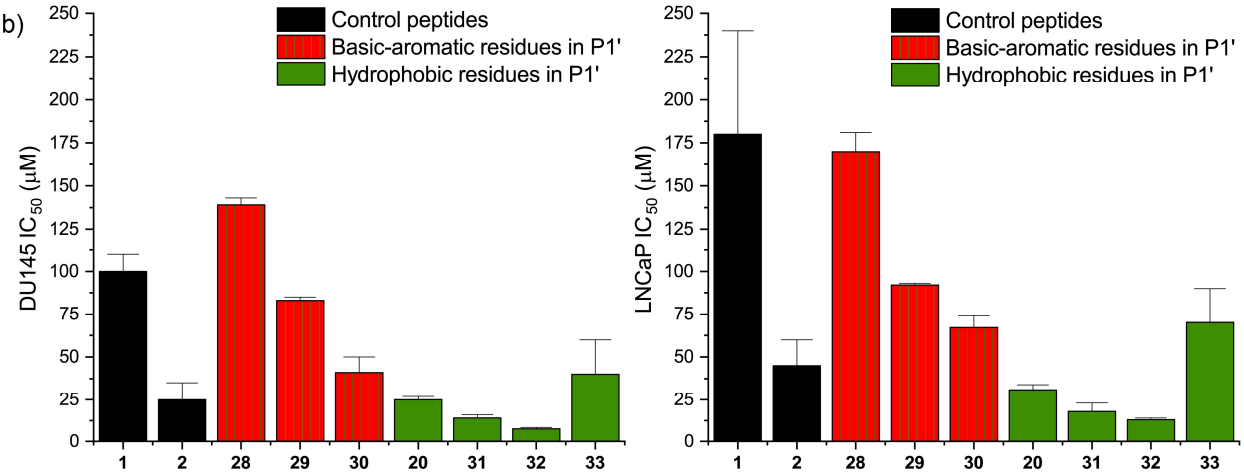

Figure 2. a) The PACE4 affinity and antiproliferative activity of compounds **28**–**33**. K_i and IC_{50} values are means of at least two independent experiments. Errors reported as SEM for K_i and IC_{50}. For more details on the concentration of inhibitors in the MTT antiproliferative assay see experimental section. b) The IC_{50} values of selected compounds for DU145 and LNCaP PCa cell lines.

Since the decarboxylated compound **30** (residue **24** at P1') showed better IC_{50} values than compounds **28** and **29**, P1'-Trp in compound **20** was replaced with tryptamine (Tryp) **25**

increasing the C-terminal hydrophobicity. As expected, compound **31** showed promising IC_{50} values (14 ± 2 μM for DU145 and 18 ± 5 μM for LNCaP cells). To further increase the cell efficacy, compound **31** was modified in P1 position by substituting Arg with (*S*)-2-amino-3-(4-carbamimidoylphenyl)propanoic acid (Acpa) **26** and (*S*)-2-amino-3-(4-carbamimidoylphenyl)acetic acid (Aca) **27** which have the 4-amidinophenyl side chain similar to Amba in compound **2**. Those modifications led to the compounds **32** (PACE4 K_i of 41 ± 7 nM) and **33** (PACE4 K_i of 248 ± 6 nM). The PACE4 affinity comparison of these compounds with compound **31** indicates a 2-fold preference for Acpa (**32**) over Arg (**31**) in P1 position while Aca (**33**) is 6 times disfavored. The diminished PACE4 affinity of compound **33** is most likely due to the steric hindrance around the opening of P1 pocket. Overall, there seems to be no correlation between affinity and antiproliferative activity linked to the nature of the P1' residues (**Figure 3-a**). On the other hand, observations indicate that such a correlation may exist at the P1 position, since PACE4 affinity is well translated into PCa cell antiproliferative activity in both compounds **32** and **33**. Compound **32**, displaying unprecedented IC_{50} values (7.5 ± 0.8 and 13 ± 1 μM for DU145 and LNCaP cells, respectively) for PCa cell lines, is a good candidate for further in vivo studies (**Figure 2-b**).

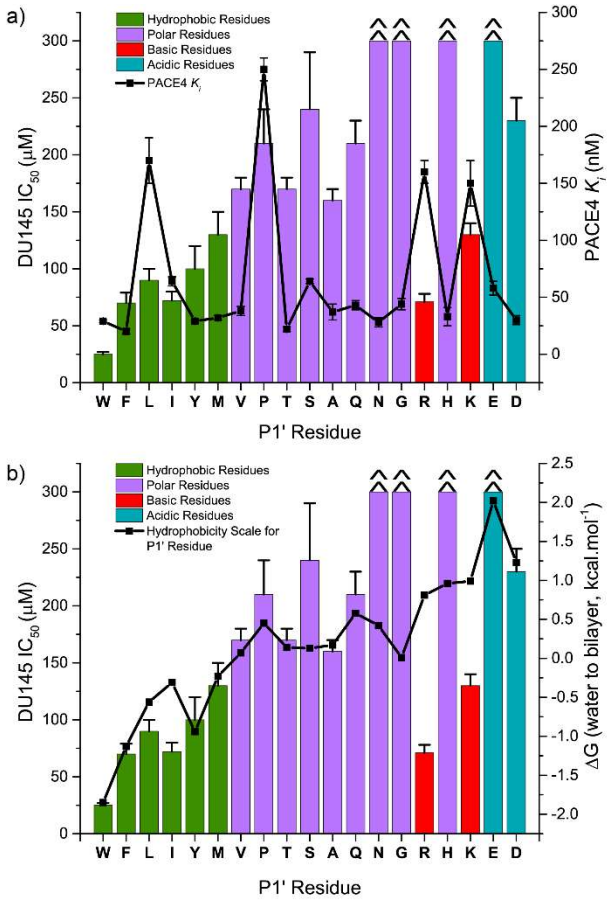

Figure 3. a) Linear relation of IC_{50} values for MTT antiproliferative assay on DU145 PCa cell line with Wimley-White bilayer scale for hydrophobicity of P1' residues and b) weak correlation to PACE4 affinity of compounds **3**–**21**.

Cell permeability studies. The relationship between K_i and IC_{50} is clearly not linear. It is obvious that PACE4 affinity of inhibitors translates poorly into antiproliferative activity with introduction of the P1' residue (**Figure 3-a**). On the other hand, there is a linear relation between hydrophobicity of P1' residues and antiproliferative activity of compounds (**Figure 3-b**). The IC_{50} values are in respectable agreement with Wimley-White bilayer scale for hydrophobicity of amino acids.[20] In this scale, the $\Delta G_{(water\ to\ bilayer)}$, is calculated for the partitioning of peptides Ac-

WL-X-LL-OH (X: natural amino acid) between water and a POPC lipid bilayer.[21] The $\Delta G_{(water\ to\ bilayer)}$ value of each amino acid can be used to evaluate its contribution to membrane penetration.

We, thus, suggest that the preeminent cytostatic activity of compounds with a hydrophobic P1'-residue originated from enhancement in penetration of such peptides through cell membrane. Thus, the compounds **35**–**38** which were FITC-labeled in their N-terminal. After an hour of incubation of the labeled compounds with DU145 cells, the emitted fluorescence from cells was analyzed using fluorescence-activated cell sorting (FACS) and compared to compound **34** as control. The signal of membrane absorbed peptides was eliminated by treatment of cells with trypan blue prior to analysis. The depicted results in **Figure 4** revealed that the higher permeability achieved with increased P1' hydrophobicity. In comparison to control compound **34**, uptake of compounds **37** and **38** enhanced by 2 and 3.5-fold, respectively, which totally correlate with IC_{50} values for compounds **20** and **31**. The better penetration of compounds with Arg (**35**) and Lys (**36**) in P1' position, compared to control, also suggests that lower PACE4 affinity of compounds **16** and **10** were compensated by their amended cell penetration.

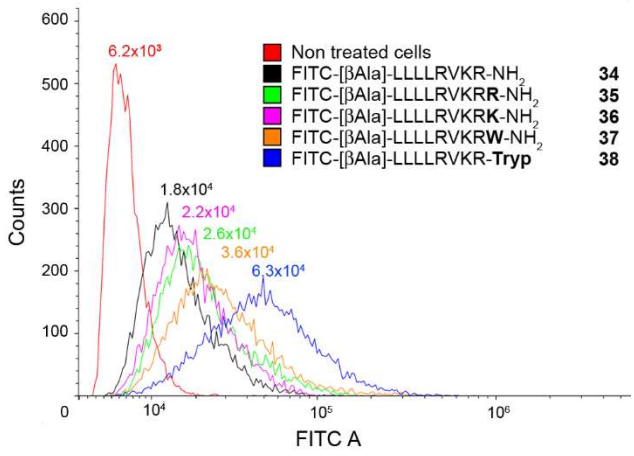

Figure 4. Quantitative cell penetration assessment of FITC-labeled compounds **35**–**38** compared to control compound **34**.

The direct relation between cell penetration and antiproliferative activity has been constantly observed for compound **1** and its derivatives.[10, 12] The cell permeability is required to reach the intracellular PACE-altCT isoform which is responsible for PACE4-associated cell growth of prostate malignant cells.[5] This is consistent with our previous observations with N-terminal PEGylated derivatives of compound **1** displayed no cell permeability and thus no antiproliferative activity.[9] The amphipathic nature of peptide inhibitors with the charged warhead and four hydrophobic residues in N-terminal has been considered crucial for cell derivatives of compound **2**.[15] Arg residues plays the key role in cell permeability of poly-arginine cell penetrating peptides (CPPs), including compound **1** derivatives, through bidentate electrostatic and hydrogen bonds with negatively charged groups of membrane.[22] Hydrophobic residues, when present in a CPP, increase the interactions with lipid bilayer and thus increasing translocation of peptides through membrane.[23] Among hydrophobic residues, inclusion of Trp within basic peptides is a molecular determinant for enhancement of cell uptake efficiency.[24-27] For instance, more abundancy of Trp residues in amphiphilic helical CPPs increased their uptake in A549 cell lines.[28] The exclusive role of tryptophan in cell penetration of polyarginine peptides is ascribed to the interaction with sulfated glycosaminoglycans possibly through hydrophobic and π–anion interactions in addition to its important hydrophobic interactions with lipid bilayer.[29-30]

DU145 cell toxicity studies. The toxicity of compounds **10**, **16**, **20**, **31** and **32** on DU145 cells was evaluated to ascertain the fact that observed fluorescence in the permeability assay is related to pure cell penetration of peptides and not to cell lysis. Hence, DU145 cells treated with peptides for 1.5 h and the number of live cells was assessed by addition of PI (propidium iodide) followed by FACS measurement of fluorescence. The compounds **10** and **16**, displayed no

toxicity to doses up to 100 μM. The results for compounds **20**, **31**, and **32** revealed that toxicity for these compounds occurred at concentrations above 10 μM which is more than 10-fold higher than the tested concentration for FITC-labeled peptides (1μM) in permeability assays (**Figure S1**). For compound **32**, a few more concentrations were tested to obtain a dose-response curve for cellular toxicity (DU145 IC_{50} (PI) = 28 ± 2 μM; **Figure 6**). In comparison, this compound inhibited metabolic activity of DU145 cells in 4-fold lower doses (DU145 IC_{50} (MTT) = 7.5 ± 0.8 μM). The fact that 4-fold more concentration of compound **32** is necessary for DU145 cytotoxicity, suggests that this compound is likely mediating its effects through mechanisms other than killing the cells in one-digit μM concentrations.

Plasma stability studies. Despite rapid tumor uptake of PACE4-inhibitor, which permits in vivo efficacy, the half-lives of all-natural residue peptide inhibitors of PACE4 in human plasma is quite short.[11] Accordingly, increasing the peptide stability in biological matrices is essential. Half-life ($t_{1/2}$) of compound **31** with DLeu in P8 and Tryp in P1' (0.8 h) was less than half of compound **2** (1.7 h). Statistically, addition of a residue in P1' increased the number of breakable amide bonds thus making the modified peptides more prone to the plasma proteases than their 8-mer counterparts. It is well known that replacement of natural residues with the unnatural one, is a way that could potentially increase the stability of peptides.[31] As a result, modification of P1-Arg in **31** with Acpa in **32** increased the plasma half-life up to 2.0 h (**Figure 5**).

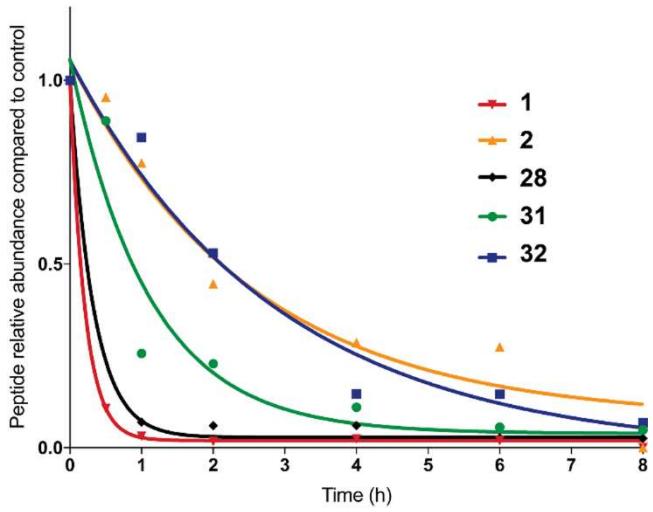

Figure 5. Stability of compounds **28**, **31** and **32** in human plasma comparing to lead compounds **1** and **2**.

Acute toxicity studies. To assess the safety profile of compound **32**, the acute toxicity of this compound was studied on healthy mice. The experiment included a single intravenous or intraperitoneal administration dose of compound **32** into healthy mice (CD1 mice as standard for toxicological and safety evaluations) at various doses to find the toxicity threshold (maximum tolerated dose, MTD). The results indicated that this compound has an MTD of at least 5 mg/kg for intravenous administration (**Figure 6-b)**.

In a previous study, we showed that a 2 mg/kg/day dose of compound **2** is sufficient for therapeutic activity in a LNCaP xenografted model of prostate cancer[11] while it displayed safe profile in acute toxicity studies (MTDs of 10 mg/kg in healthy mice).[12] The in vivo therapeutic activity for compound **32** is yet to be evaluated in LNCaP xenografted models.

a)

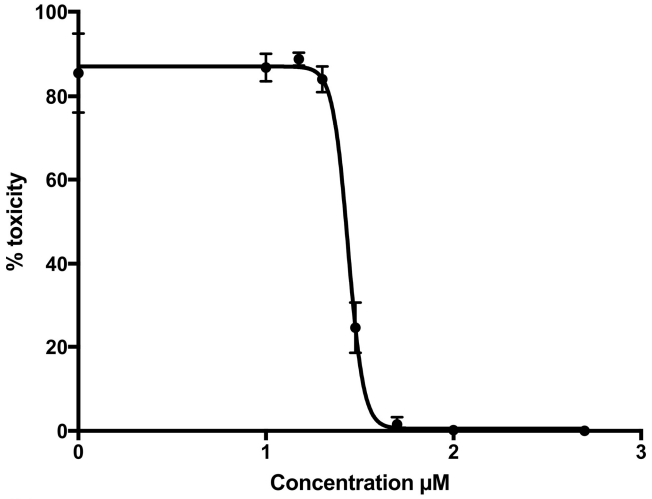

b)

Compound	IC_{50} (PI)	MTD (i.v.)
32	28 ± 2 µM	>5 mg/kg

Figure 6. The toxicity profile of compound **32**. a) The dose-response curve for DU145 cellular toxicity was performed using PI as a staining reagent. The errors are reported as SEM. For more details on concentration of inhibitors in this assay see experimental section. b) Table showing IC_{50}(PI) and MTD values of compound **32** in healthy CD1 mice. Data are representative of at least two independent experiments.

Synthesis. Compounds **3**−**21**, **28** and **29** with amino acid residues in P1' were prepared with conventional 9-fluorenylmethyloxycarbonyl (Fmoc)-based solid phase peptide synthesis (SPPS) on TentaGel® S RAM resin (**Scheme S1**). The decarboxylated analogues **30**, **31**, **32** and **33** were synthesized using a combination of solid and solution phase peptide synthesis (**Schemes 1** and **2**). At first crude protected peptide were obtained from Fmoc-SPPS on 2-chlorotrityl chloride resin, and then the free C-terminal was coupled with the corresponding amines in solution. The global deprotection with a TFA cocktail (composed of TFA/TIPS/H_2O 95:5:5) yielded the desired peptides.

Scheme 1. Synthesis of P1 residue of compound **30**, and P1-P1' adduct of compounds **32** and **33**.[a]

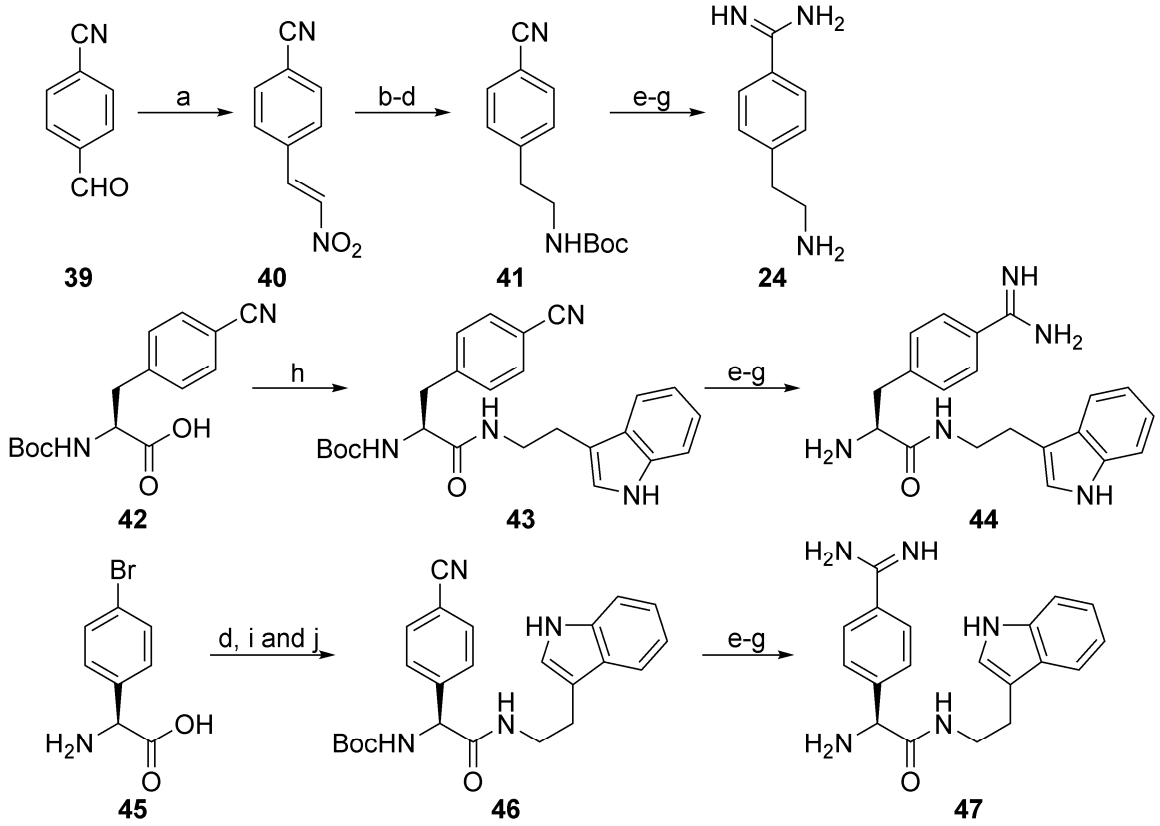

[a]Reagents and conditions: (a) CH_3NO_2, NaOH, MeOH/H_2O, <10-15 ºC, 15 min then 5 M HCl; (b) Bu_3SnH, DCM, rt, 16 h; (c) Zn, HCl(aq), 65 ºC, 1 h; (d) $(Boc)_2O$, K_2CO_3, THF/H_2O, 16 h; (e) $NH_2OH.HCl$, DIPEA, MeOH, 60 ºC, 16 h; (f) Ac_2O, DIPEA, THF then 5% Pd/C, AcOH/MeOH 35 atm H_2, 16 h; (g) Conc. HCl(aq), MeOH, 0 ºC to rt, 1 h; (h) tryptamine hydrochloride, EDCI, 6-Cl-HOBt, DIPEA, DCM, 0 ºC to rt, 16 h; (i) *i*-BuOCOCl, DIPEA, tryptamine hydrochloride, THF, −20 ºC, 2 h; (j) $Pd(PPh_3)_4$, $Zn(CN)_2$, DMF, 100 ºC, 16 h.

For obtaining Aeba **24**, aldehyde **39** condensed with nitromethane to give (*E*)-4-(2-nitrovinyl)benzonitrile **40** (**Scheme 1**). The double bond and nitro moiety were reduced using tributyltin hydride and Zn/HCl, respectively. The resulting amine was protected with *t*-butyl

carbamate (Boc) group for more convenient purification in the following steps. Transformation of nitrile **41** to amidine in compound **24** was performed as previously reported for Amba.[10] Boc-Phe(4-CN)-OH **42** was coupled with tryptamine **25** using EDCI coupling reagent. Compound **45**'s amino group was protected with Boc and then coupled with tryptamine **25** at low temperature using acyl chloride strategy. An additional cyanation step was necessary to obtain compound **46**. The conversion of nitrile groups in compounds **43** and **46** to the corresponding amidines in **44** and **47** was performed with a similar procedure as was used for AEBA **24**.

Scheme 2. Synthesis of compounds **30**−**33**.[a]

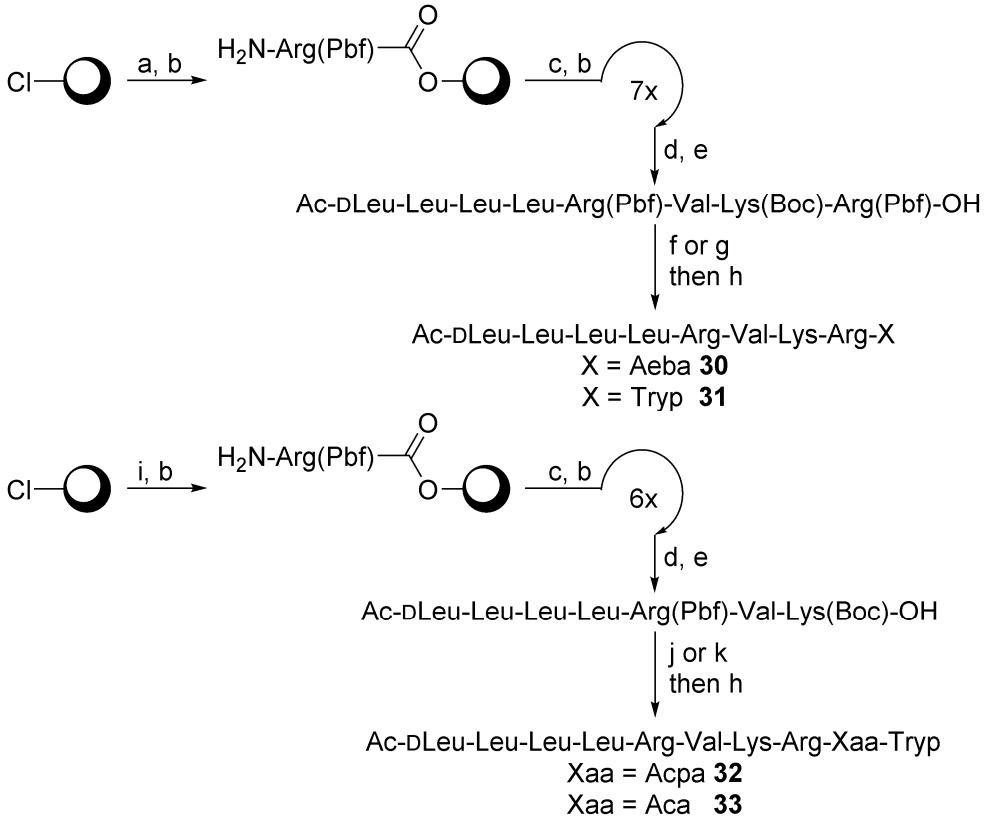

[a]Reagents and conditions: (a) Fmoc-Arg(Pbf)-OH, DIPEA, DMF/DCM (1:1); (b) Pip/DMF (1:4); (c) Fmoc-aa-OH, HATU, DIPEA, DMF; (d) Ac-DLeu-OH, HATU, DIPEA, DMF; (e) HFIP/DCM (1:4); (f) PyBOP, 6-Cl-HOBt, DIPEA, DMF, **24**, 0 °C to rt, 16 h; (g) PyBOP, 6-Cl-

HOBt, DIPEA, DMF, tryptamine hydrochloride, 0 ºC to rt, 16 h; (h) TFA/TIPS/H_2O (38:1:1); (i) Fmoc-Lys(Boc)-OH, DIPEA, DMF/DCM (1:1); (j) PyBOP, 6-Cl-HOBt, DIPEA, DMF, **44**, 0 ºC to rt, 16 h; (k) PyBOP, 6-Cl-HOBt, DIPEA, DMF, **47**, 0 ºC to rt, 16 h.

CONCLUSION

In conclusion, we developed PACE4 inhibitors by SAR studies in P1 and P1' using ML-peptide **1** as template. By performing a systematic screening of natural amino acids in P1' position of peptide **1**, compound **20** (Trp in P1') was identified as having improved antiproliferative effect on PCa cell lines. Further modification of this Trp residue to Tryp (**31**) increased the hydrophobicity in the C-terminal region of the resulting peptide. Despite its diminished affinity for recombinant PACE4, Trp to Tryp replacement improved plasma stability and cell efficacy. In an attempt to further increase the in vitro cell activity of compound **31**, P1-Arg was replaced with an Acpa residue. This change contributed to the plasma stability and antiproliferative effect of compound **32** which possesses the best cell efficacy of peptide **1** derivatives reported to date. The enhancement of antiproliferative activity with the incorporation of Trp or Tryp in the C-terminal region was found to be related to the improved cell penetration properties of such inhibitors. The cell permeability is the main obstacle in the development of multi-basic inhibitors of PACE4 as well as similar targets such as furin and some other flaviviral proteases.[32-34] The present study constitutes a significant step forward to address such cell penetration issues.

EXPERIMENTAL

Chemistry. *General Experimental Methods.* All chemical reagents and solvents were obtained from commercial resources and used without further purification. Fmoc-protected amino acids and coupling reagents, were purchased from ChemPep (Miami, FL, USA) or Chem-Impex

International (Wood Dale, IL, USA). Tryptamine and most of other reagents were bought from Sigma Aldrich (St. Louis, MO, USA). TentaGel® S RAM resin and 2-chlorotrityl-chloride resin were received from Rapp Polymer (Tübingen, Germany). Peptide synthesis (Fmoc/*t*Bu strategy) was accomplished either manually or automatically on a Pioneer peptide synthesizer (Applied Biosystems). The purification and purity check of peptide inhibitors were performed using reverse phase high-performance liquid chromatography (RP-HPLC) on an Agilent Technologies 1100 system (analytical and semi-prep) equipped with a diode array detector (λ = 210, 214, 230, and 254 nm). Preparative HPLC were done using either a Varian ProStar preparative system equipped with a UV-Vis detector (λ = 214 nm) or a Waters preparative HPLC system (Autosampler 2707, Quaternary gradient module 2535, UV detector 2489 (λ = 214 and 230 nm), fraction collector WFCIII) equipped with an ACE5 C18 column (250 × 21.2 mm, 5 μm spherical particle size). A gradient of 0.1% TFA in water and acetonitrile was used as eluent. Analytical HPLC was carried out using C18 columns, either Agilent Eclipse XDB (5 mm, 4.6 μm, 250 mm) or a Phenomenex Jupiter (5 mm, 4.6 μm, 250 mm). ESI-HRMS (TripleTOF 5600, ABSciex; Foster City, CA, USA) was used to confirm the identity of the pure products. Water H Class Acquity UPLC coupled with an SQ Detector 2 and a PDA eλ detector paired with an Acquity UPLC CSH C18 column (1.7 μm×2.1 mm×50 mm) was also used for synthesis check and plasma stability assessment (linear gradient from 5 to 95% of ACN containing 0.1% formic acid in 0.1% aqueous formic acid was used for 1.3 min, flow rate 0.8 mL/min). NMR experiment were performed on either AV300 Bruker (300 MHz for ^{1}H and 75 MHz for ^{13}C) or an Avance III hd 400 Bruker (400 MHz for ^{1}H and 100 MHz for ^{13}C). ^{13}C NMR experiments were done with complete decoupling of protons. Infrared (IR) spectra were recorded using Alpha-Platinum ATR Bruker, diamond crystal.

Peptide Synthesis. A sequence of washes including DMF 3×, a cycle of MeOH/DCM 3× and DCM 3× was applied, after every reaction on resin except stated otherwise. TentaGel® S RAM resin was used for the synthesis of compounds **3**−**21**, **28** and **29**. The chain length growth was performed by standard Fmoc-SPPS. Fmoc group was removed with 20% piperidine in DMF. Fmoc protected amino acids were coupled using 5 equiv of protected amino acids, 5 equiv of HATU and 15 equiv of DIPEA in DMF. The cleavage from resin and side chain deprotection was carried out in one step with a cocktail of TFA/TIPS/H_2O 95:2.5:2.5 for 2 h. The crude peptides were triturated with Et_2O after evaporation of 50% of cleaving cocktail, centrifuged and the supernatant was discarded. For compounds **30**−**33** the peptide cores were synthesized on 2-chlorotrtiyl chloride resin as following. 1.2 equiv of first amino acid was loaded on resin in the presence of 4 equiv DIPEA in DMF for 3 h. The unreacted groups were capped with a mixture of DCM/MeOH/DIPEA 85:10:5. Resin, then, was washed by a sequence of DCM 3×, a cycle of MeOH/DCM 3× and DCM 5×. The protected peptides were cleaved from resin with 20% hexafluoro-2-propanol in DCM. The solvent was evaporated in vacuo and the residue was dissolved in a mixture of *t*-BuOH/H_2O (1:1) and lyophilized. A mixture of protected peptide, 2.5 equiv of corresponding P1' or P1-P1' amine, 2.2 equiv of PyBOP, 7.5 equiv of 6-Cl-HOBt was dissolved in DMF and cooled in an ice bath, then 7.5 equiv of DIPEA was added to the solution and the reaction was stirred overnight. Solvent was removed with an air stream and the crude protected peptide was deprotected with the same TFA cocktail as compounds **3**−**21**. FITC-labeled peptides were prepared as reported elsewhere.[10] The crude of compounds **3**−**21**, **28**−**33** and **35**−**38** were purified using preparative HPLC. Analytical HPLC was used for confirmation of purity (>95%) of fractions. These compounds were characterized by high-resolution mass

spectroscopy (HRMS). The HPLC chromatograms and HRMS details of these compounds are provided in supplementary material.

(*E*)-4-(2-Nitrovinyl)benzonitrile (40). A solution of NaOH (0.84 g, 21.00 mmol) in ice-water (40 mL) was added dropwise to a solution of 4-Formylbenzonitrile (2.60 g, 20.00 mmol) and $MeNO_2$ (1.08 mL, 20.00 mmol) in MeOH (40 mL). The reaction temperature was kept below 10-15 °C during the addition of the NaOH solution. After stirring for 15 min, the whole reaction mixture was transferred to a separating funnel and slowly added to 5 M HCl (100 mL). A yellow solid was obtained almost instantly. The solid was filtered, washed with cold water, dried and recrystallized from hot EtOH to furnish the title compound as yellow crystal needles (1.66 g, 48%). ^{1}H NMR (400 MHz, $CDCl_3$) δ (ppm): 8.00 (d, J = 13.7 Hz, 1H), 7.77 (d, J = 8.4 Hz, 2H), 7.67 (d, J = 8.4 Hz, 2H), 7.62 (d, J = 13.7 Hz, 1H). ^{13}C NMR (100 MHz, $CDCl_3$) δ (ppm) 139.5, 136.5, 134.4, 133.0, 129.4, 117.8, 115.3.

***tert*-Butyl (4-cyanophenethyl)carbamate (41).** The first step was adopted from a literature method with some modifications[35]. To a solution of compound **40** (1.29 g, 7.40 mmol) in dry DCM (19 mL) under inert atmosphere was added tributyltin hydride (2.39 mL, 8.88 mmol) and the reaction mixture was stirred for 16 h. After completion of reaction, the solvent was evaporated under reduced pressure. The residue was partitioned between MeCN (100 mL) and hexanes (30 mL). The MeCN phase was then washed two more times with hexanes to remove the remained tin biproducts and concentrated under reduced pressure. The residue was dissolved in MeOH (110 mL) and 2 N HCl (110 mL). Zinc powder (6.00 g, 90.00 mmol) was added slowly to the solution prior to stirring for 1 h at 65 °C, it was cooled and basified to pH 8 with sodium carbonate. The solids were filtered off and the filtrate was concentrated to half of its volume. To this solution was added $(Boc)_2O$ (1.62 g, 7.44 mmol) in THF (50 mL) and stirred overnight.

After completion of reaction, THF was evaporated under reduced pressure and the product was extracted with EtOAc three times. The combined organic phases were washed with brine, dried over magnesium sulfate and evaporated to dryness. Flash chromatography with hexanes/EtOAc (5:1 to 4:1) as eluent furnish title compound as a colorless crystalline solid (1.13 g, 57% for three step). ^{1}H NMR (300 MHz, $CDCl_3$) δ (ppm): 7.59 (d, J = 8.0 Hz, 2H), 7.30 (d, J = 8.0 Hz, 2H), 4.60 (br. s., 1H), 3.38 (ABq, J = 6.5 Hz, 2H), 2.86 (t, J = 6.5 Hz, 2H), 1.42 (s, 9 H). ^{13}C NMR (75 MHz, $CDCl_3$) δ (ppm) 155.7, 144.7, 132.3, 129.6, 118.8, 110.3, 79.5, 41.3, 36.4, 28.3. HRMS (ESI) calculated for $C_{14}H_{18}N_2O_2$ m/z $[M+H]^+$ 247.1441 found 247.1415.

4-(2-Aminoethyl)benzimidamide (24). To a solution of **41** (0.27 g, 1.07 mmol) in MeOH (20 mL) was added hydroxylammonium chloride (0.11 g, 1.60 mmol) and DIPEA (0.28 mL, 1.60 mmol) and the reaction was stirred at room temperature overnight. The solvent was evaporated under reduced pressure after 16 h stirring at 60 ºC and the residue was taken into EtOAc, washed with water and brine and dried over magnesium sulfate. The solvent was evaporated in vacuum and the residue dissolved in THF (10 mL). DIPEA (0.28 mL, 1.60 mmol) and acetic anhydride (0.15 mL, 1.60 mmol) were added to the solution. The amidoxime were acetylated within 30 min according to TLC. Then, the volatiles were evaporated in vacuo and the residue was dissolved in EtOAc, washed with 0.50 M HCl and brine, dried over magnesium sulfate and the solvent removed in vacuo. Then the residue was dissolved in 1:1 MeOH/ AcOH and 5% Pd/C (0.050 g) were added. The hydrogenation was conducted under 35 atm pressure of H_2 in a Parr hydrogenator jar for 16 h. After the completion of reaction (HPLC-MS) reaction mixture was passed through a pad of diatomaceous earth and purified with preparative HPLC (gradient of 0 to 30% MeCN in water) to yield a white solid. (0.19 g, 69%). ^{1}H NMR (300 MHz, D_2O) δ (ppm): 7.76 (d, J = 8.0 Hz, 1H), 7.51 (d, J = 8.0 Hz, 1H), 3.41 (t, J = 7.0 Hz, 1H), 3.09 (t, J = 7.0 Hz,

1H). ^{13}C NMR (75 MHz, DMSO-*d*6) δ (ppm) 165.3, 144.0, 129.3, 128.4, 126.1, 39.2, 32.7 HRMS (ESI) calculated for $C_9H_{13}N_3$ m/z $[M+H]^+$ 264.1706 found 264.1683. The obtained solid was, then, dissolved in MeOH (3 mL) and conc. HCl (1 mL) was added slowly in 0 ºC. After stirring for 1 h the solvent was evaporated by an argon stream. The residue was triturated using MeOH/Et_2O to achieve a white solid in quantitative yield. ^{1}H NMR (400 MHz, DMSO-*d*$_6$) δ (ppm): 9.34 (s, 2H), 8.40 (br. s., 2H), 7.87 (d, *J* = 8.4 Hz, 2H), 7.51 (d, *J* = 8.4 Hz, 2H), 3.00-3.09 (m, 4H). ^{13}C NMR (100 MHz, DMSO-*d*6) δ (ppm) 165.3, 144.0, 129.3, 128.4, 126.1, 39.2, 32.7. HRMS (ESI) calculated for $C_9H_{13}N_3$ m/z $[M+H]^+$ 164.1182 found 164.1181.

***tert*-Butyl (*S*)-(1-((2-(1H-indol-2-yl)ethyl)amino)-3-(4-cyanophenyl)-1-oxopropan-2-yl)-carbamate (43).** To a suspension of Boc-Phe(4-CN)-OH **42** (1.45 g, 5.00 mmol), tryptamine hydrochloride (0.98 g, 5.00 mmol) and 6-Cl-HOBt (0.93 g, 5.50 mmol) in DCM (15 mL) was added DIPEA (2.61 mL, 15.00 mmol) while the temperature kept 0-5 ºC. Once a clear solution obtained, EDCI (1.05 g, 5.50 mmol) was added in the same temperature. The resulting solution was stirred for 16 h at room temperature. Then, solvent was evaporated, and the residue was taken into EtOAc and washed with 10% citric acid, saturated $NaHCO_3$ and brine, then, dried over $MgSO_4$. The residue was triturated with DCM and hexanes to obtain the pure title compound as a white solid (1.96 g, 90% yield) ^{1}H NMR (400 MHz, DMSO-*d*$_6$) δ (ppm) 10.81 (br. s., 1H), 8.05 (br. s., 1H), 7.72 (d, *J* = 7.7 Hz, 2H), 7.54 (d, *J* = 7.8 Hz, 1H), 7.42 (d, *J* = 7.7 Hz, 2H), 7.34 (d, *J* = 7.8 Hz, 1H), 7.15 (s, 1H), 7.07 (t, *J* = 7.8 Hz, 1H), 6.91 - 7.02 (overlapped, 2H), 4.18 (m, 1H), 3.35 (m, 2H), 3.00 (dd, *J* = 13.0, 3.1 Hz, 1H), 2.80 (overlapped, 3H), 1.28 (s, 9H). ^{13}C NMR (100 MHz, DMSO-*d*$_6$) δ (ppm) 171.0, 155.2, 144.5, 136.3, 131.9, 130.4, 127.2, 122.7, 121.0, 119.1, 118.3, 111.7, 111.4, 109.1, 78.1, 55.3, 41.2, 37.9, 28.1, 25.1. IR (neat) ν

(cm^{-1}) 1651, 1682, 2228, 2918, 2956, 3327, 3348, 3407, 3412. HRMS (ESI) calculated for $C_{25}H_{28}N_4O_3$ m/z $[M+H]^+$ 433.2234 found 433.2306. mp; 174-176 ºC.

(*S*)-*N*-(2-(1H-indol-2-yl)ethyl)-2-amino-3-(4-cyanophenyl)propanamide (44). This compound was prepared in similar conditions that was used for **24**. ^{1}H NMR (400 MHz, D_2O) δ (ppm) 7.68 (d, *J* = 8.5 Hz, 2H), 7.56 (d, *J* = 7.9 Hz, 1H), 7.42 (d, *J* = 8.5 Hz, 2H), 7.33 (d, *J* = 7.9, 1H), 7.08 - 7.12 (m, 1H), 7.06 (s, 1H), 6.97-7.03 (m, 1H), 4.30 (dd, *J* = 9.0, 5.6 Hz, 1H), 3.42 - 3.57 (m, 2H), 3.13 (dd, *J* = 13.5, 5.6 Hz, 1H), 2.92 (t, *J* = 7.0 Hz, 2H), 2.86 (dd, *J* = 13.5, 9.0 Hz, 1H). ^{13}C NMR (100 MHz, D_2O) δ (ppm) 168.3, 157.6, 146.3, 138.3, 131.6, 129.0, 127.9, 123.6, 122.5, 119.8, 119.4, 116.9, 113.2, 112.4, 57.2, 41.4, 39.4, 26.3. IR (neat) ν (cm^{-1}) 1666, 1678, 2905, 2943, 2989, 3296, 3393, 3413 HRMS (ESI) calculated for $C_{20}H_{23}N_5O$ m/z $[M+H]^+$ 350.1975 found 350.1995. mp; decomposed at >300 ºC.

***tert*-Butyl (*S*)-(2-((2-(1H-indol-3-yl)ethyl)amino)-1-(4-cyanophenyl)-2-oxoethyl)carbamate (46).** Compounds **45** (0.92 g, 4.00 mmol) and K_2CO_3 (0.55 g, 4.00 mmol) were dissolved in H_2O (50 mL). $(Boc)_2O$ (1.05 g, 4.80 mmol) in THF (25 mL) was added to this solution and stirred overnight. After completion of reaction, THF was evaporated under reduced pressure. The solution neutralized with solid citric acid and the product was extracted to EtOAc three times. The combined organic phases were washed with brine, dried over magnesium sulfate and evaporated to dryness to give Boc-Phg(4-Br)-OH in quantitative yield. This white solid (1.38 g, 4.00 mmol) and *i*-butyl chloroformate (0.52 mL, 4.00 mmol) were dissolved in THF (20 mL) and cooled to -20 ºC prior to addition of DIPEA (0.70 mL, 4.00 mmol, precooled to -20 ºC). The suspension was agitated for 10 min before the addition of a mixture of tryptamine hydrochloride (0.94 g, 4.80 mmol) and DIPEA (0.84 mL, 4.8 mmol) in THF (5 mL). After stirring for 24 h in -20 ºC, the solvent was evaporated to dryness and the residue was partitioned between EtOAc and

water. The phases were separated, and the organic phase was washed with saturated $NaHCO_3$, water, 10% citric acid and brine solutions. The EtOAc was evaporated in vacuum and the residue was purified with flash chromatography to yield Boc-Phg(4-Br)-Tryp as a white solid (1.13 g, 60 %) ^{1}H NMR (400 MHz, $CDCl_3$) δ (ppm) 8.19 (br. s, 1H), 7.49 (d, *J* = 8.00 Hz, 1H), 7.38 (d, *J* = 8.0 Hz, 2H), 7.35 (d, *J* = 8.0 Hz, 1H), 7.20 (t, *J* = 8.0 Hz, 1H), 7.06-7.15 (overlapped, 3H), 6.68 (d, *J* = 2.2 Hz, 1H), 5.93 (overlapped, 2H), 5.02 (br. s, 1H), 3.58 (dt, *J* = 13.0, 6.5 Hz, 1H), 3.49 (dt, *J* = 13.0, 6.5 Hz, 1H), 2.80 - 2.96 (m, 2H), 1.40 (s, 9H). ^{13}C NMR (100 MHz, $CDCl_3$) δ (ppm) 169.4, 155.1, 137.7, 136.3, 131.9, 128.7, 127.0, 122.2, 122.1, 119.4, 118.4, 112.1, 111.3, 80.2, 57.9, 39.9, 28.2, 24.9. HRMS (ESI) calculated for $C_{23}H_{26}BrN_3O_3$ m/z $[M+H]^+$ 472.1230 found 472.1217. The obtained solid plus $Zn(CN)_2$ (0.16 g, 1.40 mmol) and $Pd(PPh_3)_4$ (0.13 g, 0.11 mmol) were suspended in deoxygenated dry DMF (3 mL) under inert condition. The yellow slurry was heated to 100 ºC for 16 h, then taken into EtOAc and washed three times with 20% NH_4OH, dried over $MgSO_4$, and purified with flash chromatography to yield the title compound as a white solid (0.39 g, 40%) ^{1}H NMR (400 MHz, $CDCl_3$) δ (ppm) 8.07 (br. s, 1H), 7.46 - 7.57 (overlapped, 3H), 7.38 (d, *J* = 8.0 Hz, 1H), 7.31 (d, *J* = 8.0 Hz, 2H), 7.23 (t, *J* = 8.0 Hz, 1H), 7.12 (t, *J* = 8.0 Hz, 1 H), 6.79 (d, *J* = 2.0 Hz, 1H), 5.94 (br. s, 1H), 5.76 (br. s, 1H), 5.05 (br. s, 1H), 3.57-3.67 (m, 2H), 2.84 - 2.98 (m, 2H), 1.40 (br. s., 9H). ^{13}C NMR (100 MHz, $CDCl_3$) δ (ppm) 168.5, 164.8, 143.8, 136.3, 132.6, 127.7, 127.0, 122.4, 122.0, 119.7, 118.4, 118.4, 112.1, 112.0, 111.4, 80.5, 60.4, 40.1, 28.2, 24.8. IR (neat) ν (cm^{-1}) 1659, 1699, 2235, 2939, 2983, 3234, 3290, 3421. HRMS (ESI) calculated for $C_{24}H_{26}N_4O_3$ m/z $[M+H]^+$ 419.2077 found 419.2137. mp; 98-101 ºC.

(*S*)-*N*-(2-(1H-Indol-3-yl)ethyl)-2-amino-2-(4-carbamimidoylphenyl)acetamide 47. The title compound was prepared with the same procedure as **24**. ^{1}H NMR (400 MHz, D_2O) δ (ppm) 7.54

(d, J = 8.54 Hz, 2H), 7.44 (d, J = 7.86 Hz, 1H), 7.39 (d, J = 8.20 Hz, 1H), 7.26 - 7.33 (m, 2H), 7.16 (t, J = 7.2 Hz, 1H), 7.02 (t, J = 7.2 Hz, 1H), 6.89 (s, 1H), 5.00 (s, 1H), 3.89 (ddd, J = 13.6, 8.7, 5.1 Hz, 1H), 3.39 (dt, J = 13.6, 5.1 Hz, 1H), 2.94 (dt, J = 13.6, 5.1 Hz, 1H), 2.83 (ddd, J = 13.6, 8.7, 5.1 Hz, 1H). ^{13}C NMR (100 MHz, D_2O) δ (ppm) 165.6, 162.8,137.5, 135.9, 128.5, 128.1, 126.9, 123.1, 121.6,118.9, 118.2, 114.9, 111.5, 111.0, 55.8, 39.5, 23.5. IR (neat) ν (cm^{-1}) 1622, 1682, 2914, 2970, 3010, 3265, 3292. HRMS (ESI) calculated for $C_{19}H_{21}N_5O$ m/z $[M+H]^+$ 336.1819 found 336.1872. mp; decomposed at >300 ºC.

Enzyme kinetics. The fluorometric K_i measurements of PC enzymes was performed using a Gemini EM 96-well spectrofluorometer (Molecular Devices; Sunnyvale, CA, USA) ($\lambda_{EX.}$, 370 nm; $\lambda_{EM.}$, 460 nm; Cut Off, 435 nm). Both PACE4 and furin are human recombinant produced from S2 insect cells and purified by a method described earlier[19]. All the experiments were done in duplicate or triplicate. Furin inhibition measurements were performed in 100 mM of HEPES buffer (pH = 7.5), 1 mM $CaCl_2$, 1 mM β-mercaptoethanol, and 1.8 g/L BSA, while PACE4 inhibition assays were done in a 20 mM Bis-Tris buffer (pH = 6.5), 1 mM $CaCl_2$, and 1.8 g/L BSA. The competitive substrate was pyroGlu-Arg-Thr-Lys-Arg-AMC peptide (Bachem, Switzerland) for both furin and PACE4 with the concentration of 100 μM in each well. Inhibitors were added with various concentrations in the range of 0-10 μM. 2 units of enzyme (final concentration 100 μL) were added in each well, and the real-time fluorescence was measured during 1 h of experiments. The K_i values were determined using Cheng and Prusoff's equation by SoftMaxPro5 program.[36]

Cell proliferation. MTT antiproliferative assay has been accomplished for DU145 and LNCaP PCa cell lines as reported earlier.[9] The 96 well plates seeded with approximate density of 1500 cells for DU145 or 2500 cells for LNCaP. The media was changed after 24 h followed by

addition of different concentrations of peptide inhibitors (For peptides **3−19**, **21** and **28**, a range of 300, 200, 100, 50, 25, 10 and 1 μM concentrations; and for peptides **20** and **29−33** a range of 150, 100, 75, 50, 25, 10 and 1 μM were applied). The incubation continued for 72 h prior to addition of MTT reagent (with final concentration per well of 1 g/L). The incubation continued for further 4 h. At the time, the media has been removed and cells were treated with 0.10 mL of 2-propanol/HCl (24:1 N) to solubilize the formazan produced in the mitochondria. The metabolic activity of cells assessed relatively by vehicle treated cells (Sterile bi-distilled water 0.1% DMSO). The maintenance of cells and all the assay steps were performed in RPMI 1640 5% FBS for DU145 and 10% FBS for LNCaP cells. The IC_{50} values were calculated using Prism 6.0 (GraphPad software).

Cell permeability. The DU145 cells were plated at a density of 200000 cells per 100 mm petri dish and incubated for 48 h at 37 ºC. Cells were treated with 1 μM of FITC analogs for 1 h at the same temperature prior to collection using 0.05% trypsin which later was inactivated with FBS-containing media. Cell pellets were washed one more time with PBS and were resuspended in 200 μL of fresh PBS after centrifugation. PI was added at a final concentration of 10 μg/mL just before doing the acquisition. In another set of tubes, fluorophore was quenched using trypan blue at a final concentration of 0.04%. Cells were analyzed (at least 10000 events) by CytoFLEX 15 flow cytometer (Beckman Coulter, Brea, CA, USA) with following diode lasers: 488 nm and 638 nm, 50 mW each. The emitted fluorescence was split into four channels and detected through band pass filters (Forward scatter area, side scattered area and side scattered width signals) to establish the live gates and exclude debris and cell clumps. Dead cells (PI-positive) were excluded by the gating in the red channel.

Cell toxicity. 200 000 cellules were plated in a 6-well plate and then, were treated with 1, 10, 50 and 100 μM concentrations of compounds **10**, **16**, **20** and **31** in serum free media for 1.5 h (For compound **32** the concentrations were 1, 10, 15, 20, 30, 50, 100 μM). Cells were collected using trypsin prior to washing and then resuspension in PBS. PI at a final concentration of 10 μg/mL was added just prior to acquisition of fluorescence by CytoFLEX 15 flow cytometer as described above. The IC_{50}(PI) value for compound **32** was calculated using Prism 6.0 (GraphPad software).

Plasma stability. Peptide samples for determination of $t_{1/2}$ half-lives were prepared as follows; The total concentration of 50 μM peptide in human serum (from male AB plasma; Sigma Aldrich) were incubated at 37 ºC. At each indicated timepoint and just following peptide addition, 25 μL of plasma were precipitated with 100 μL of MeOH containing 20 μM Fmoc-Leu-OH as internal standard. Samples, then, were subjected to centrifuge at 12000 ×g for 10 min at room temperature to remove precipitated proteins and clear supernatants were filtered on 0.2 μM PVDF centrifugal filters (Canadian Life Science) prior to analysis. Quantitative analysis performed based on the peptide/standard ratio of integrated area under the curve in the total ion chromatogram and reported from 0 h incubation. The one-phase decay curve-fit of GraphPad Prism was used to determine $t_{1/2}$ values.

In vivo acute toxicity. All experimental procedures were performed as reported earlier in accordance with regulations of the Canadian Council on Animal Care.[12]

ASSOCIATED CONTENT

Supporting Information

Information for enzyme kinetics and cell toxicity assays, analytical data (HPLC and HRMS analysis) and molecular formula strings for all biologically tested compounds (**3**–**21**, **28**–**33** and

35−**38**) and NMR spectra for small molecule intermediates are provided as supporting information. This material is available free of charge via the http://pubs.acs.org.

AUTHOR INFORMATIONS

Corresponding Authors

*(R.D.) Telephone: +1 (819) 821-8000, ext. 75428. E-mail: Robert.Day@USherbrooke.ca and *(Y.L.D.) Telephone: +1 (819) 821 8000 ext. 75299. E-mail: Yves.Dory@USherbrooke.ca

ORCID

Vahid Dianati: **0000-0001-6883-6574**

Anna Kwiatkowska: **0000-0002-5659-3680**

Yves Dory: **0000-0003-4758-1589**

Robert Day: **0000-0001-8123-1991**

Notes

The authors declare no competing financial interest.

ACKNOWLEDGMENTS

We acknowledge the Canadian Cancer Society Research Institute (701590 to R.D. and Y.L.D.) and Prostate Cancer Canada (TAG2014-02 to R.D.) for their support. F.C. holds a Banting and Charles Best Canada Graduate Scholarships (grant#315690) from CIHR and Graduate Studentship from Prostate Cancer Canada (Grant #GS-2015-07). We also thank Hugo Gagnon and Jean-Philippe Couture (PhenoSwitch Biosciences Inc.) for HRMS analysis and Sandra Gagnon for acute toxicity analysis.

ABBREVIATIONS USED

PC, proprotein convertase; PCa, prostate cancer; PACE4, paired basic amino acid cleaving enzyme 4; GDF-15, Growth/differentiation factor 15; Amba, 4-amidinobenzylamide; *S*-*i*-Agb,

(2*S*)-amino-(3*S*)-guanidinobutyryl; CPP, cell penetrating peptide; MTT, 3-(4,5-dimethylthiazol-2-yl)-2,5-diphenyltetrazolium bromide; Apa, 4-aminophenylalanine; Gpa, 4-guanidinophenylalanine; Aeba, 4-(2-aminoethyl)benzimidamide; Tryp, tryptamine; Acpa, (*S*)-2-amino-3-(4-carbamimidoylphenyl)propanoic acid; Aca, (*S*)-2-amino-3-(4-carbamimidoylphenyl)acetic acid; POPC, 1-palmitoyl-2-oleoyl-sn-glycero-3-phosphocholine; FACS, fluorescence-activated cell sorting; FITC, fluorescein isothiocyanate; SPPS, solid phase peptide synthesis; DIPEA, *N,N*-diisopropylethylamine; NMM, *N*-methylmorpholine; 6-Cl-HOBt, 6-chloro-1-hydroxybenzotriazole; HFIP, hexafluoro-2-propanol; PyBOP, benzotriazol-1-yl-oxytripyrrolidino-phosphonium hexafluorophosphate; AMC, 7-amido-4-methylcoumarin; HATU, 1-[bis(dimethylamino)methylene]-1*H*-1,2,3-triazolo[4,5-*b*]pyridinium 3-oxid hexafluorophosphate; EDCI, 1-ethyl-3-(3-dimethylaminopropyl)carbodiimide; FBS, fetal bovine serum; PI, propidium iodide.

REFERENCES

(1) Mains, R. E.; Berard, C. A.; Denault, J. B.; Zhou, A.; Johnson, R. C.; Leduc, R., Pace4: A Subtilisin-Like Endoprotease with Unique Properties. *Biochem. J.* **1997**, *321*, 587−593.

(2) Klein-Szanto, A. J.; Bassi, D. E., Proprotein Convertase Inhibition: Paralyzing the Cell's Master Switches. *Biochem. Pharmacol.* **2017**, *140*, 8−15.

(3) D'Anjou, F.; Routhier, S.; Perreault, J. P.; Latil, A.; Bonnel, D.; Fournier, I.; Salzet, M.; Day, R., Molecular Validation of Pace4 as a Target in Prostate Cancer. *Transl. Oncol.* **2011**, *4*, 157−172.

(4) Couture, F.; D'Anjou, F.; Desjardins, R.; Boudreau, F.; Day, R., Role of Proprotein Convertases in Prostate Cancer Progression. *Neoplasia* **2012**, *14*, 1032−1042.

(5) Couture, F.; Sabbagh, R.; Kwiatkowska, A.; Desjardins, R.; Guay, S.-P.; Bouchard, L.; Day, R., Pace4 Undergoes an Oncogenic Alternative Splicing Switch in Cancer. *Cancer Res.* **2017**, *77*, 6863−6879.

(6) Lin, Y.-E.; Wu, Q.-N.; Lin, X.-D.; Li, G.-Q.; Zhang, Y.-J., Expression of Paired Basic Amino Acid-Cleaving Enzyme 4 (Pace4) Correlated with Prognosis in Non-Small Cell Lung Cancer (Nsclc) Patients. *J. Thorac. Dis.* **2015**, *7*, 850−860.

(7) Longuespée, R.; Couture, F.; Levesque, C.; Kwiatkowska, A.; Desjardins, R.; Gagnon, S.; Vergara, D.; Maffia, M.; Fournier, I.; Salzet, M.; Day, R., Implications of Proprotein Convertases in Ovarian Cancer Cell Proliferation and Tumor Progression: Insights for Pace4 as a Therapeutic Target. *Transl. Oncol.* **2014**, *7*, 410−419.

(8) Panet, F.; Couture, F.; Kwiatkowska, A.; Desjardins, R.; Guérin, B.; Day, R., Pace4 Is an Important Driver of Zr-75-1 Estrogen Receptor-Positive Breast Cancer Proliferation and Tumor Progression. *Eur. J. Cell Biol.* **2017**, *96*, 469−475.

(9) Levesque, C.; Fugere, M.; Kwiatkowska, A.; Couture, F.; Desjardins, R.; Routhier, S.; Moussette, P.; Prahl, A.; Lammek, B.; Appel, J. R.; Houghten, R. A.; D'Anjou, F.; Dory, Y. L.; Neugebauer, W.; Day, R., The Multi-Leu Peptide Inhibitor Discriminates between Pace4 and Furin and Exhibits Antiproliferative Effects on Prostate Cancer Cells. *J. Med. Chem.* **2012**, *55*, 10501−10511.

(10) Kwiatkowska, A.; Couture, F.; Levesque, C.; Ly, K.; Desjardins, R.; Beauchemin, S.; Prahl, A.; Lammek, B.; Neugebauer, W.; Dory, Y. L.; Day, R., Design, Synthesis, and Structure-Activity Relationship Studies of a Potent Pace4 Inhibitor. *J. Med. Chem.* **2014**, *57*, 98−109.

(11) Levesque, C.; Couture, F.; Kwiatkowska, A.; Desjardins, R.; Guerin, B.; Neugebauer, W. A.; Day, R., Pace4 Inhibitors and Their Peptidomimetic Analogs Block Prostate Cancer Tumor

Progression through Quiescence Induction, Increased Apoptosis and Impaired Neovascularisation. *Oncotarget* **2015**, *6*, 3680−3693.

(12) Kwiatkowska, A.; Couture, F.; Levesque, C.; Ly, K.; Beauchemin, S.; Desjardins, R.; Neugebauer, W.; Dory, Y. L.; Day, R., Novel Insights into Structure-Activity Relationships of N-Terminally Modified Pace4 Inhibitors. *ChemMedChem* **2016**, *11*, 289−301.

(13) Lepek, T.; Kwiatkowska, A.; Couture, F.; Ly, K.; Desjardins, R.; Dory, Y.; Prahl, A.; Day, R., Macrocyclization of a Potent Pace4 Inhibitor: Benefits and Limitations. *Eur. J. Cell Biol.* **2017**, *96*, 476−485.

(14) Kwiatkowska, A.; Couture, F.; Ait-Mohand, S.; Desjardins, R.; Guérin, B.; Day, R. unpublished results. It is important to mention that in our previous studies (Ref. 12) half-life ($t_{1/2}$) values were reported based on a method using 0.50 g/L concentrations of peptides. The high concentrations of peptides could potentially inhibit some proteases and/or compete for the degradation. In the present study, we utilized a more sensitive method based on UPLC-MS detection, which allows us to reduce the final concentration of peptides to 50 μg/L thus obtaining more reliable half times. Obviously, the obtained results for two methods are incomparable.

(15) Maluch, I.; Levesque, C.; Kwiatkowska, A.; Couture, F.; Ly, K.; Desjardins, R.; Neugebauer, W. A.; Prahl, A.; Day, R., Positional Scanning Identifies the Molecular Determinants of a High Affinity Multi-Leucine Inhibitor for Furin and Pace4. *J. Med. Chem.* **2017**, *60*, 2732−2744.

(16) Dianati, V.; Shamloo, A.; Kwiatkowska, A.; Desjardins, R.; Soldera, A.; Day, R.; Dory, Y. L., Rational Design of a Highly Potent and Selective Peptide Inhibitor of Pace4 by Salt Bridge Interaction with D160 at Position P3. *ChemMedChem* **2017**, *12*, 1169−1172.

(17) Henrich, S.; Lindberg, I.; Bode, W.; Than, M. E., Proprotein Convertase Models Based on the Crystal Structures of Furin and Kexin: Explanation of Their Specificity. *J. Mol. Biol.* **2005**, *345*, 211−227.

(18) Basak, A.; Koch, P.; Dupelle, M.; Fricker, L. D.; Devi, L. A.; Chretien, M.; Seidah, N. G., Inhibitory Specificity and Potency of Prosaas-Derived Peptides toward Proprotein Convertase 1. *J. Biol. Chem.* **2001**, *276*, 32720−32728.

(19) Fugere, M.; Limperis, P. C.; Beaulieu-Audy, V.; Gagnon, F.; Lavigne, P.; Klarskov, K.; Leduc, R.; Day, R., Inhibitory Potency and Specificity of Subtilase-Like Pro-Protein Convertase (Spc) Prodomains. *J. Biol. Chem.* **2002**, *277*, 7648−7656.

(20) Wimley, W. C.; White, S. H., Experimentally Determined Hydrophobicity Scale for Proteins at Membrane Interfaces. *Nat. Struct. Biol.* **1996**, *3*, 842−848.

(21) White, S. H.; Wimley, W. C., Hydrophobic Interactions of Peptides with Membrane Interfaces. *BBA-Rev. Biomembranes* **1998**, *1376*, 339−352.

(22) Futaki, S.; Nakase, I., Cell-Surface Interactions on Arginine-Rich Cell-Penetrating Peptides Allow for Multiplex Modes of Internalization. *Acc. Chem. Res.* **2017**, *50* , 2449−2456.

(23) Bechara, C.; Sagan, S., Cell-Penetrating Peptides: 20years Later, Where Do We Stand? *FEBS Lett.* **2013,** *587*, 1693−1702.

(24) Rydberg, H. A.; Matson, M.; Åmand, H. L.; Esbjörner, E. K.; Nordén, B., Effects of Tryptophan Content and Backbone Spacing on the Uptake Efficiency of Cell-Penetrating Peptides. *Biochemistry* **2012**, *51*, 5531−5539.

(25) Maiolo, J. R.; Ferrer, M.; Ottinger, E. A., Effects of Cargo Molecules on the Cellular Uptake of Arginine-Rich Cell-Penetrating Peptides. *BBA-Biomembranes* **2005,** *1712*, 161−172.

(26) Eksteen, J. J.; Ausbacher, D.; Simon-Santamaria, J.; Stiberg, T.; Cavalcanti-Jacobsen, C.; Wushur, I.; Svendsen, J. S.; Rekdal, Ø., Iterative Design and in Vivo Evaluation of an Oncolytic Antilymphoma Peptide. *J. Med. Chem.* **2017**, *60*, 146−156.

(27) Hung, L.-C.; Jiang, I.; Chen, C.-J.; Lu, J.-Y.; Hsieh, Y.-F.; Kuo, P.-H.; Hung, Y.-L.; Wang, L. H.-C.; Chang, M. D.-T.; Sue, S.-C., Heparin-Promoted Cellular Uptake of the Cell-Penetrating Glycosaminoglycan Binding Peptide, Gbpecp, Depends on a Single Tryptophan. *ACS Chem. Biol.* **2017**, *12*, 398−406.

(28) Jafari, M.; Karunaratne, D. N.; Sweeting, C. M.; Chen, P., Modification of a Designed Amphipathic Cell-Penetrating Peptide and Its Effect on Solubility, Secondary Structure, and Uptake Efficiency. *Biochemistry* **2013**, *52*, 3428−3435.

(29) Bechara, C.; Pallerla, M.; Zaltsman, Y.; Burlina, F.; Alves, I. D.; Lequin, O.; Sagan, S., Tryptophan within Basic Peptide Sequences Triggers Glycosaminoglycan-Dependent Endocytosis. *FASEB J.* **2013**, *27*, 738−749.

(30) Mascotti, D. P.; Lohman, T. M., Thermodynamics of Charged Oligopeptide-Heparin Interactions. *Biochemistry* **1995**, *34*, 2908−2915.

(31) Luca, G.; Rossella De, M.; Lucia, C., Chemical Modifications Designed to Improve Peptide Stability: Incorporation of Non-Natural Amino Acids, Pseudo-Peptide Bonds, and Cyclization. *Curr. Pharm. Design* **2010**, *16*, 3185−3203.

(32) Kouretova, J.; Hammamy, M. Z.; Epp, A.; Hardes, K.; Kallis, S.; Zhang, L.; Hilgenfeld, R.; Bartenschlager, R.; Steinmetzer, T., Effects of Ns2b-Ns3 Protease and Furin Inhibition on West Nile and Dengue Virus Replication. *J. Enzym. Inhib. Med. Chem.* **2017**, *32*, 712−721.

(33) Weigel, L. F.; Nitsche, C.; Graf, D.; Bartenschlager, R.; Klein, C. D., Phenylalanine and Phenylglycine Analogues as Arginine Mimetics in Dengue Protease Inhibitors. *J. Med. Chem.* **2015**, *58*, 7719−7733.

(34) Stoermer, M. J.; Chappell, K. J.; Liebscher, S.; Jensen, C. M.; Gan, C. H.; Gupta, P. K.; Xu, W.-J.; Young, P. R.; Fairlie, D. P., Potent Cationic Inhibitors of West Nile Virus Ns2b/Ns3 Protease with Serum Stability, Cell Permeability and Antiviral Activity. *J. Med. Chem.* **2008**, *51*, 5714−5721.

(35) Palomo, C.; Aizpurua, J. M.; Cossio, F. P.; Garcia, J. M.; Lopez, M. C.; Oiarbide, M., Tributyltin Hydride Addition to Nitroalkenes: A Convenient Procedure for the Conversion of Nitroalkenes into Nitroalkanes and Carbonyl Compounds. *J. Org. Chem.* **1990,** *55*, 2070−2078.

(36) Cheng, Y.; Prusoff, W. H., Relationship between the Inhibition Constant (K_I) and the Concentration of Inhibitor Which Causes 50 Percent Inhibition (I_{50}) of an Enzymatic Reaction. *Biochem. Pharmacol.* **1973**, *22* (23), 3099−3108.

TOC Graphic:

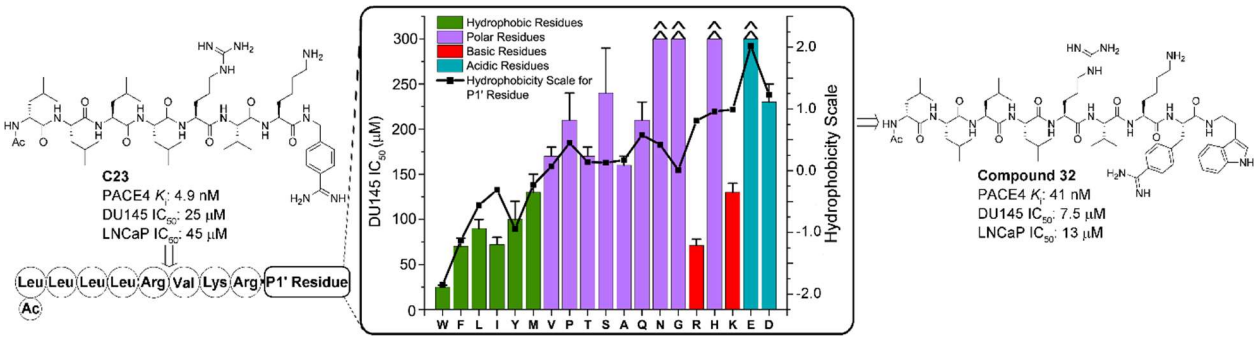

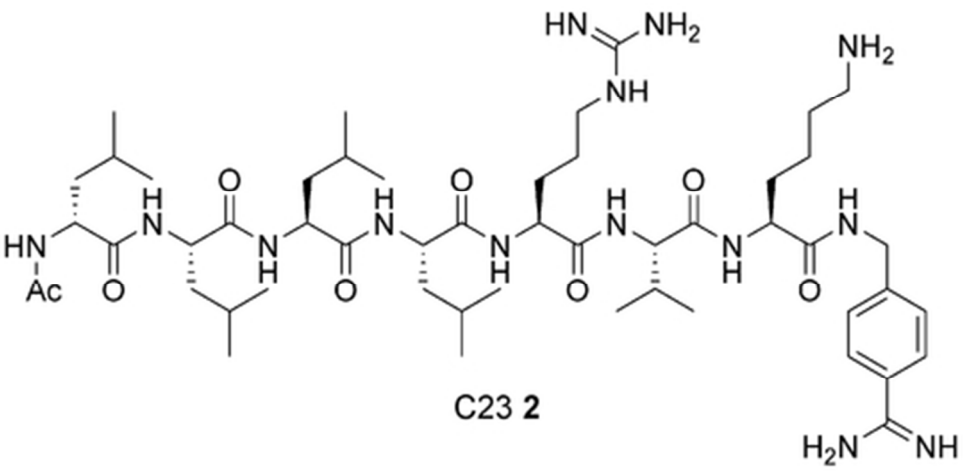

Figure 1. Structure of lead compound **2** (C23)

40x19mm (300 x 300 DPI)

a)

Entry	Structure	K_i (nM) ± SEM		Selectivity for PACE4	IC_{50} (μM) ± SEM	
		PACE4	Furin		DU145	LNCaP
28	Ac-Leu-Leu-Leu-Leu-Arg-Val-Lys-Arg-**Apa**-NH_2	32 ± 4	130 ± 10	4	139 ± 4	170 ± 10
29	Ac-Leu-Leu-Leu-Leu-Arg-Val-Lys-Arg-**Gpa**-NH_2	11 ± 2	140 ± 10	13	83 ± 2	92 ± 2
30	Ac-**D**Leu-Leu-Leu-Leu-Arg-Val-Lys-Arg-**Aeba**	68 ± 1	700 ± 100	10	41 ± 9	67 ± 7
31	Ac-**D**Leu-Leu-Leu-Leu-Arg-Val-Lys-Arg-**Tryp**	70 ± 10	280 ± 2	4	14 ± 2	18 ± 5
32	Ac-**D**Leu-Leu-Leu-Leu-Arg-Val-Lys-Arg-**Acpa**-**Tryp**	41 ± 5	80 ± 10	2	7.5 ± 0.8	13 ± 1
33	Ac-**D**Leu-Leu-Leu-Leu-Arg-Val-Lys-Arg-**Aca**-**Tryp**	248 ± 6	3000 ± 500	12	40 ± 20	70 ± 20

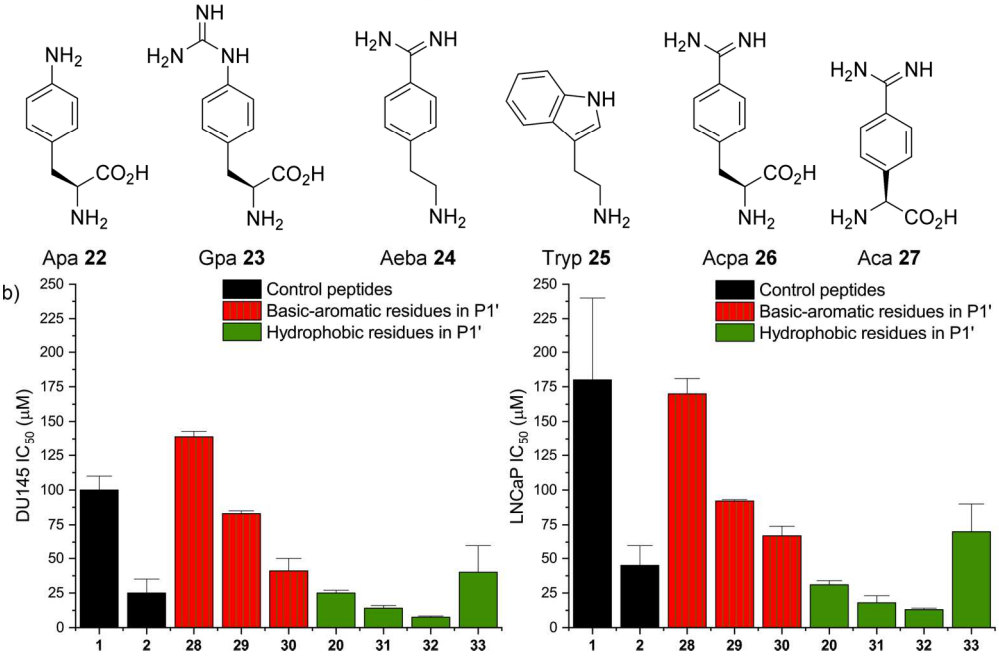

Figure 2. a) The PACE4 affinity and antiproliferative activity of compounds **28–33**. K_i and IC_{50} values are means of at least two independent experiments. Errors reported as SEM for K_i and IC_{50}. For more details on the concentration of inhibitors in the MTT antiproliferative assay see experimental section. b) The IC_{50} values of selected compounds for DU145 and LNCaP PCa cell lines.

161x150mm (300 x 300 DPI)

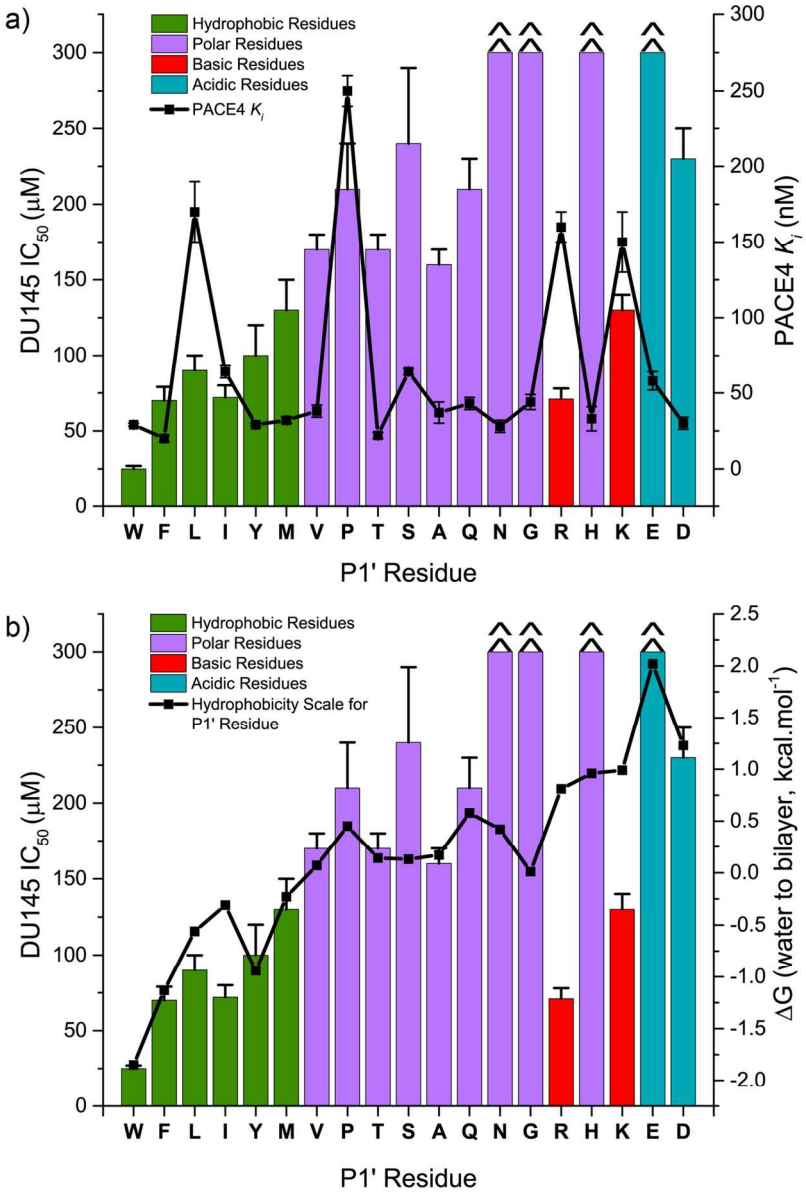

Figure 3. a) Linear relation of IC_{50} values for MTT antiproliferative assay on DU145 PCa cell line with Wimley-White bilayer scale for hydrophobicity of P1' residues and b) weak correlation to PACE4 affinity of compounds **3–21**.

119x168mm (300 x 300 DPI)

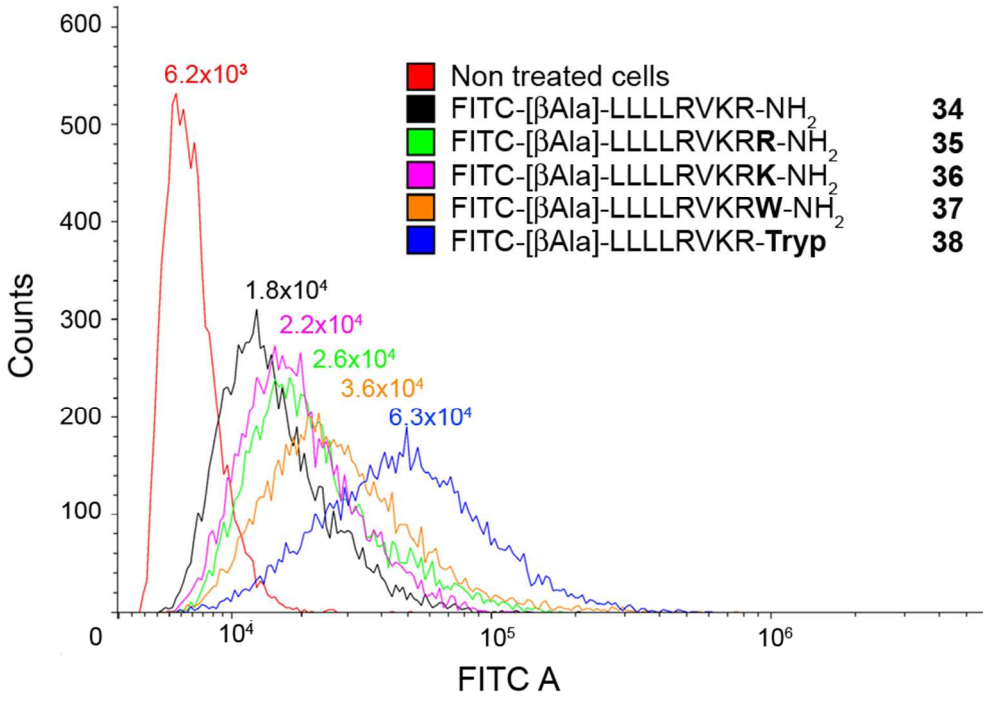

Figure 4. Quantitative cell penetration assessment of FITC-labeled compounds **35–38** compared to control compound **34**.

84x62mm (300 x 300 DPI)

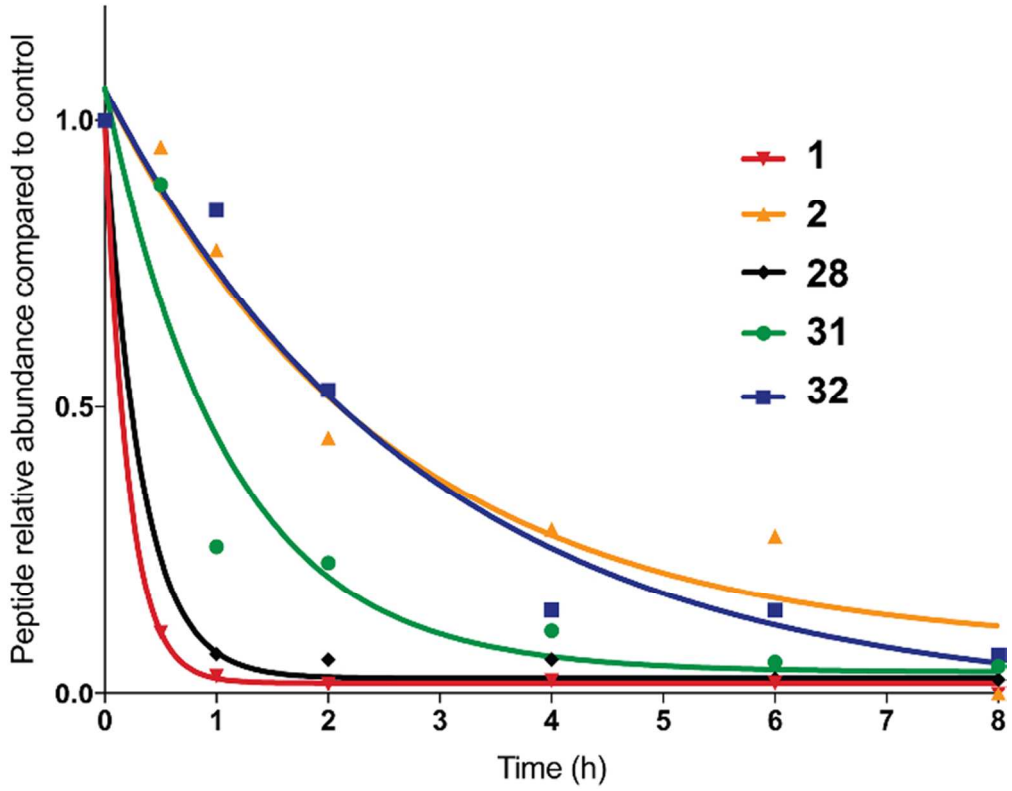

Figure 5. Stability of compounds **28**, **31** and **32** in human plasma comparing to lead compounds **1** and **2**.

84x66mm (300 x 300 DPI)

a)

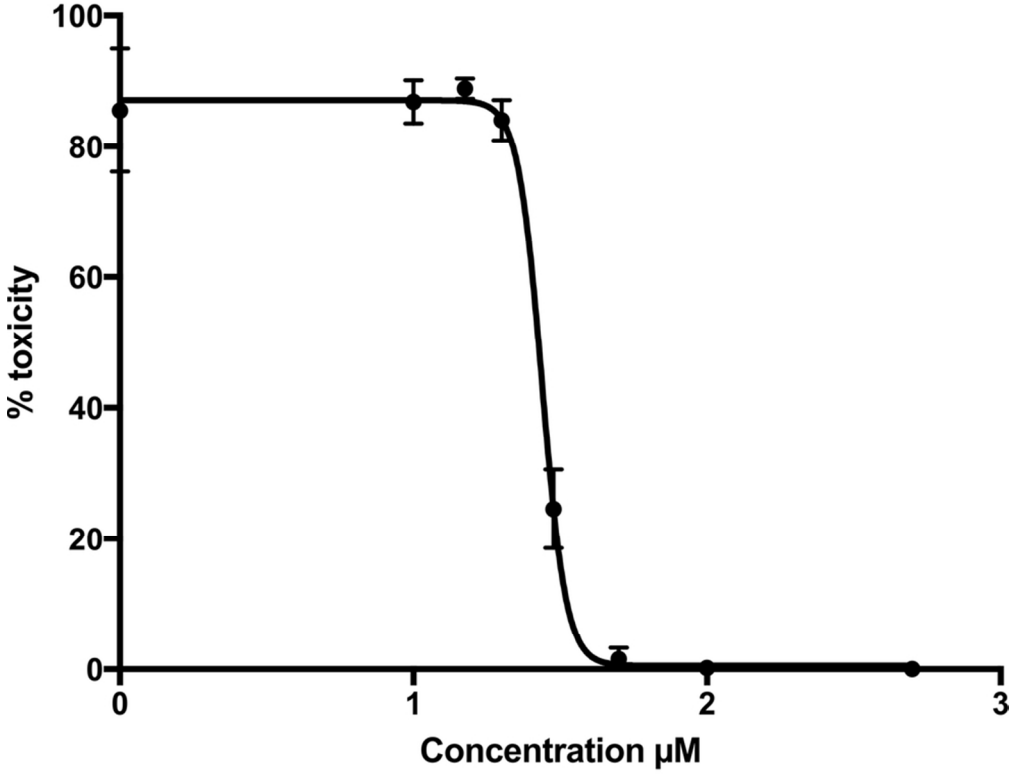

b)

Compound	IC_{50} (PI)	MTD (i.v.)
32	28 ± 2 μM	>5 mg/kg

Figure 6. The toxicity profile of compound **32**. a) The dose-response curve for DU145 cellular toxicity was performed using PI as a staining reagent. The errors are reported as SEM. For more details on concentration of inhibitors in this assay see experimental section. b) Table showing IC_{50}(PI) and MTD values of compound **32** in healthy CD1 mice. Data are representative of at least two independent experiments.

83x81mm (300 x 300 DPI)

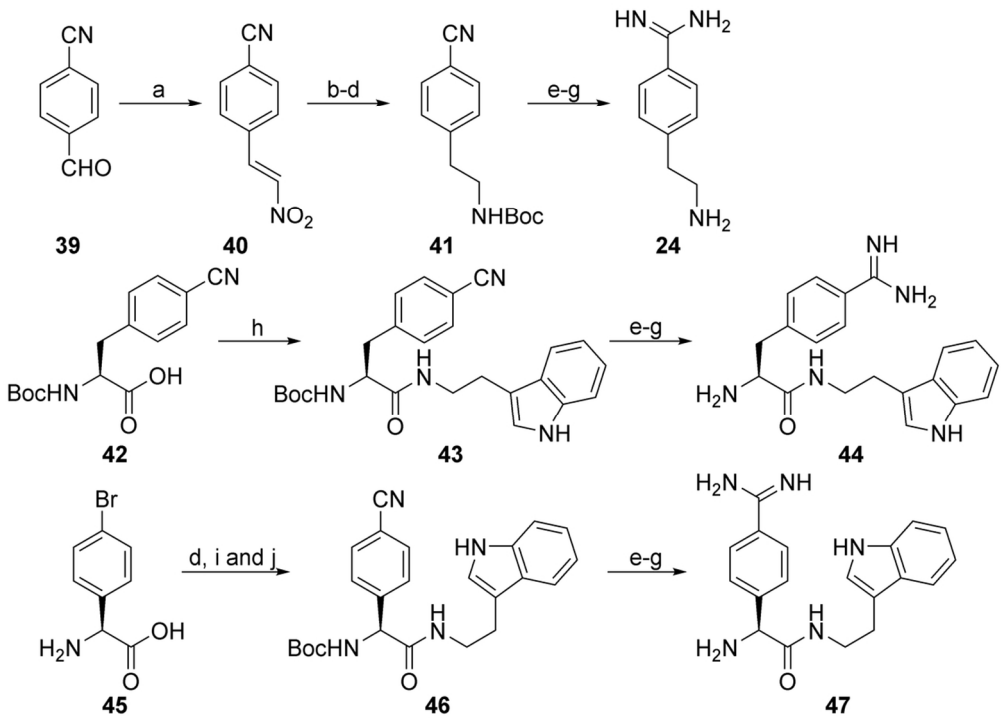

Scheme 1. Synthesis of P1 residue of compound **30**, and P1-P1' adduct of compounds **32** and **33**.[a]

110x79mm (300 x 300 DPI)

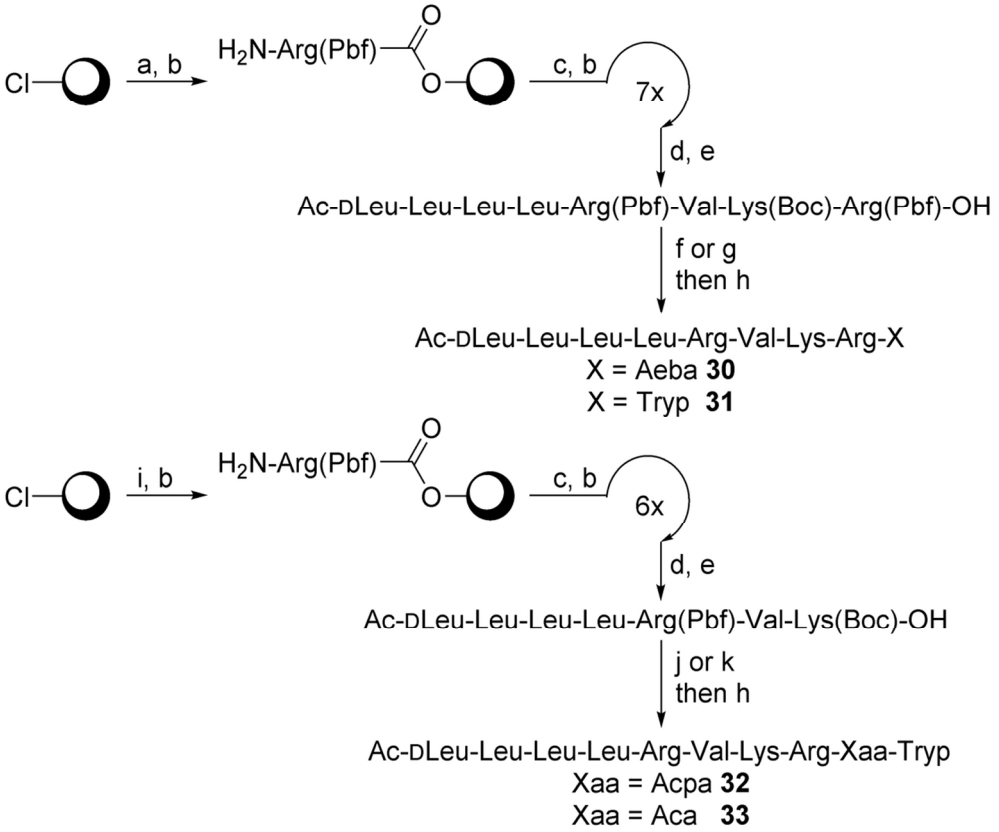

Scheme 2. Synthesis of compounds **30–33**.[a]

109x92mm (300 x 300 DPI)

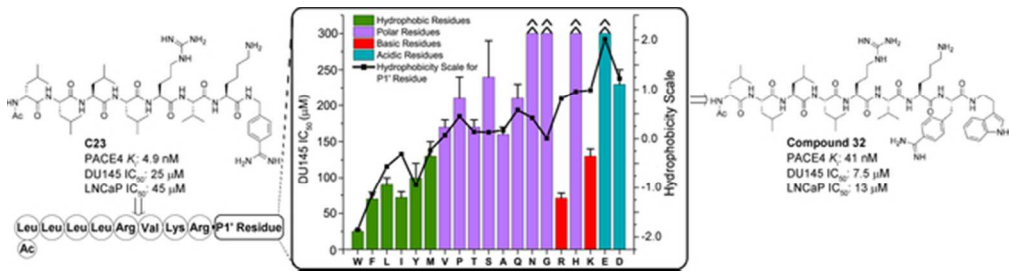

54x14mm (300 x 300 DPI)